A search for main-belt comets in the Palomar Transient Factory survey

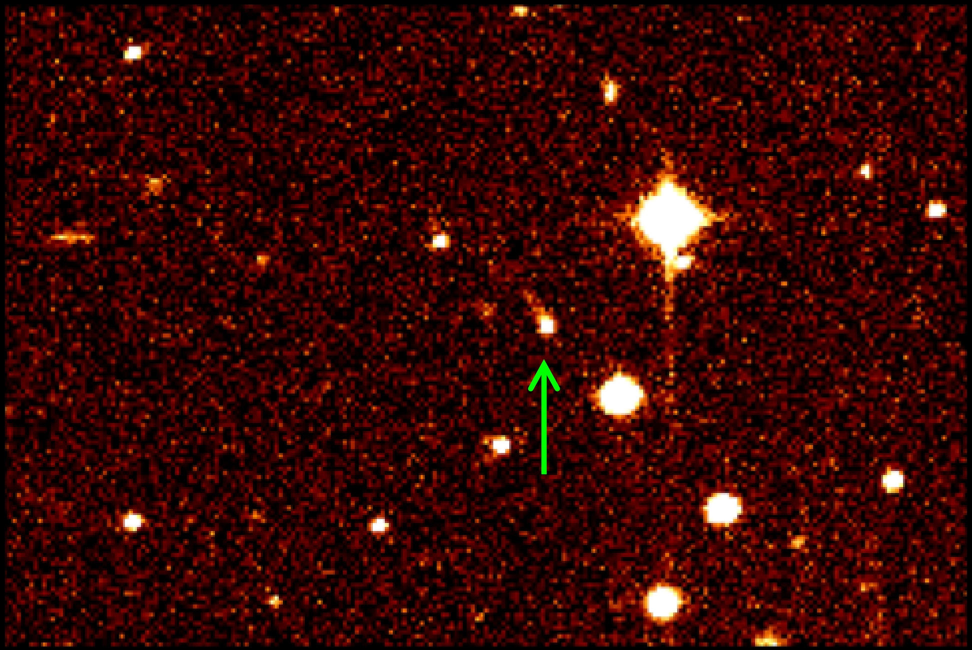

Adam Waszczak[1], Eran O. Ofek[2], Oded Aharonson[1,3], Shrinivas R. Kulkarni[4], David Polishook[5], James M. Bauer[6], David B. Levitan[4], Branimir Sesar[4], Russ Laher[6], Jason Surace[6] and the PTF Team

[1]Division of Geological and Planetary Sciences, California Institute of Technology, Pasadena, CA
[2]Benoziyo Center for Astrophysics, Faculty of Physics, Weizmann Institute of Science, Rehovot, Israel
[3]Helen Kimmel Center for Planetary Science, Weizmann Institute of Science, Rehovot, Israel
[4]Division of Mathematics, Physics and Astronomy, California Institute of Technology, Pasadena, CA
[5]Department of Earth, Atmospheric and Planetary Sciences, Massachusetts Institute of Technology, Cambridge, MA
[6]Jet Propulsion Laboratory, California Institute of Technology, Pasadena, CA
[7]Spitzer Science Center, California Institute of Technology, Pasadena, CA

Remote-observation-based classification

observable	**comets**	**asteroids**
appearance (image)	extended, diffuse	point-source
composition (spectrum)	ice-bearing	not ice-bearing
orbital type	excited (large a, e, i)	stable (small a, e, i)

Remote-observation-based classification

comets | **asteroid**

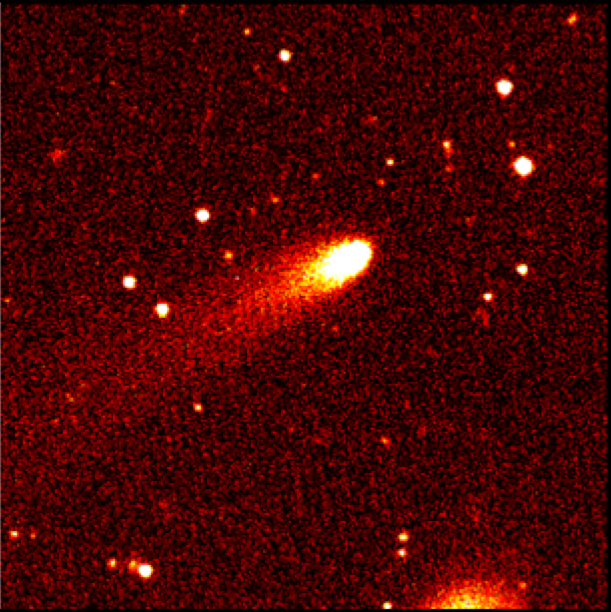

260P/McNaught

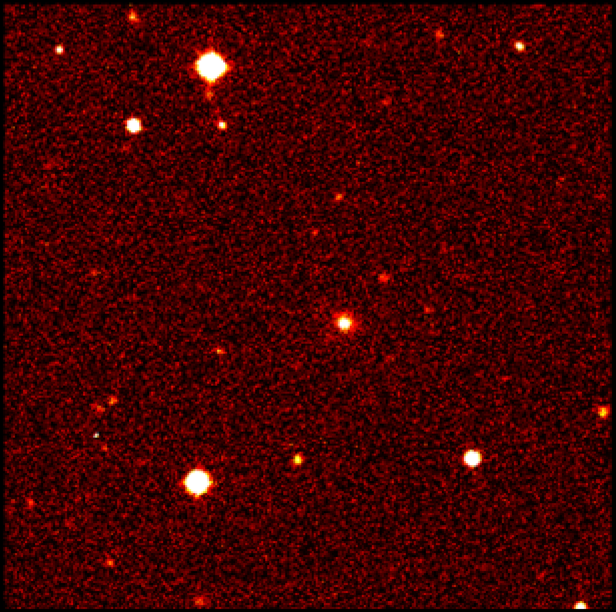

2011 CR42

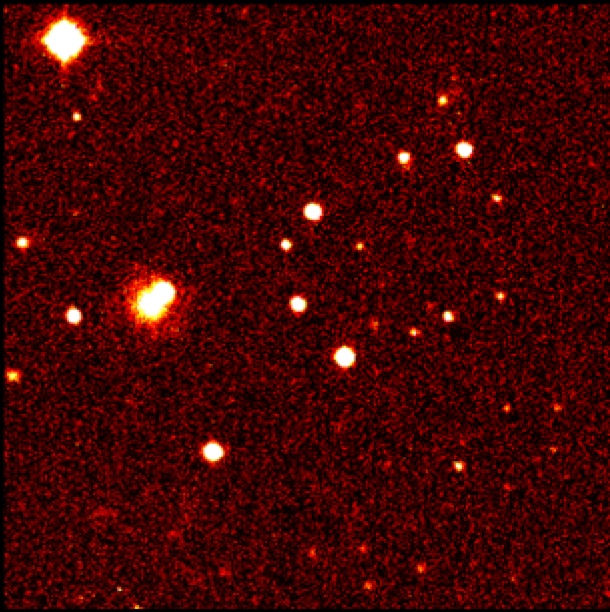

2309 Mr. Spock

Jenniskins 2006, in *Meteors and their parent comets*

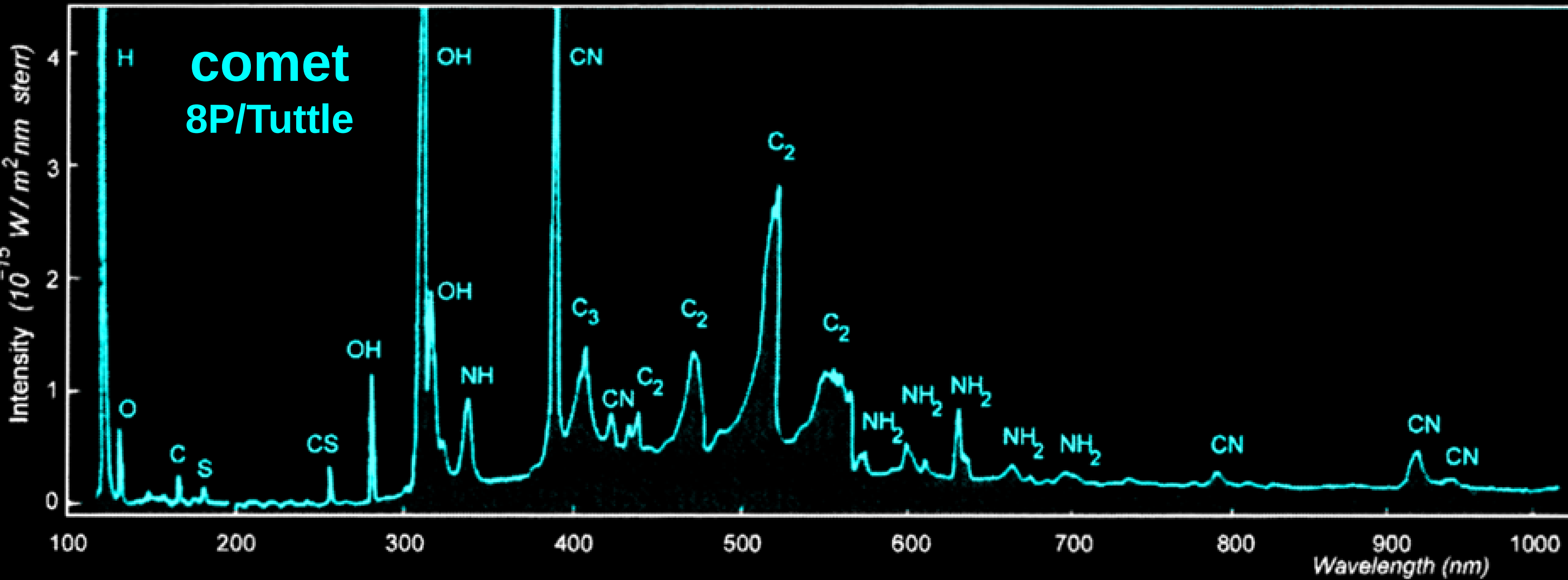

Bus et al. 2003, in *Asteroids II*

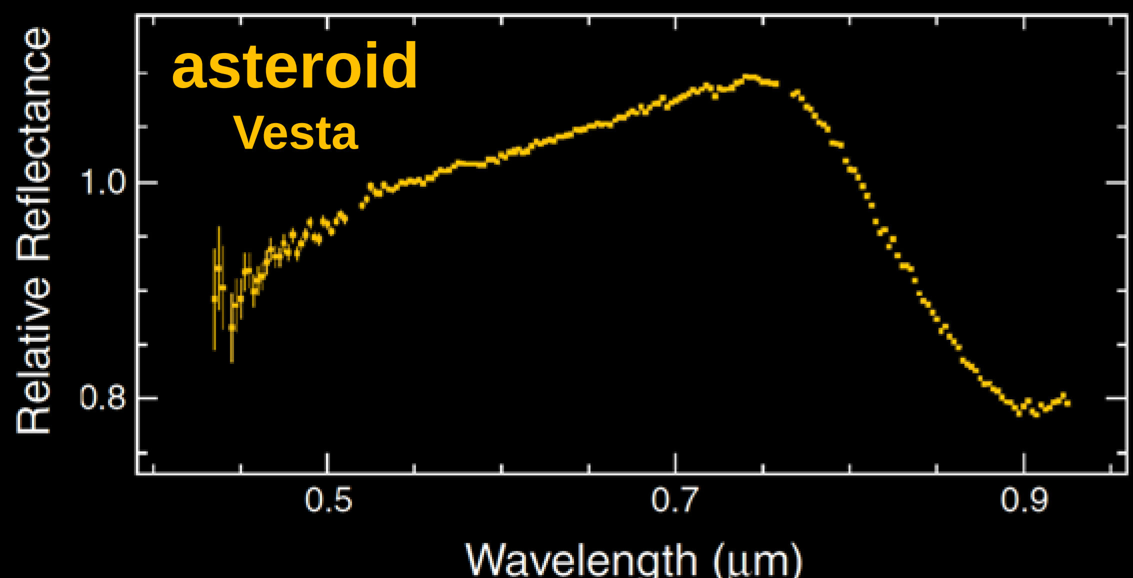

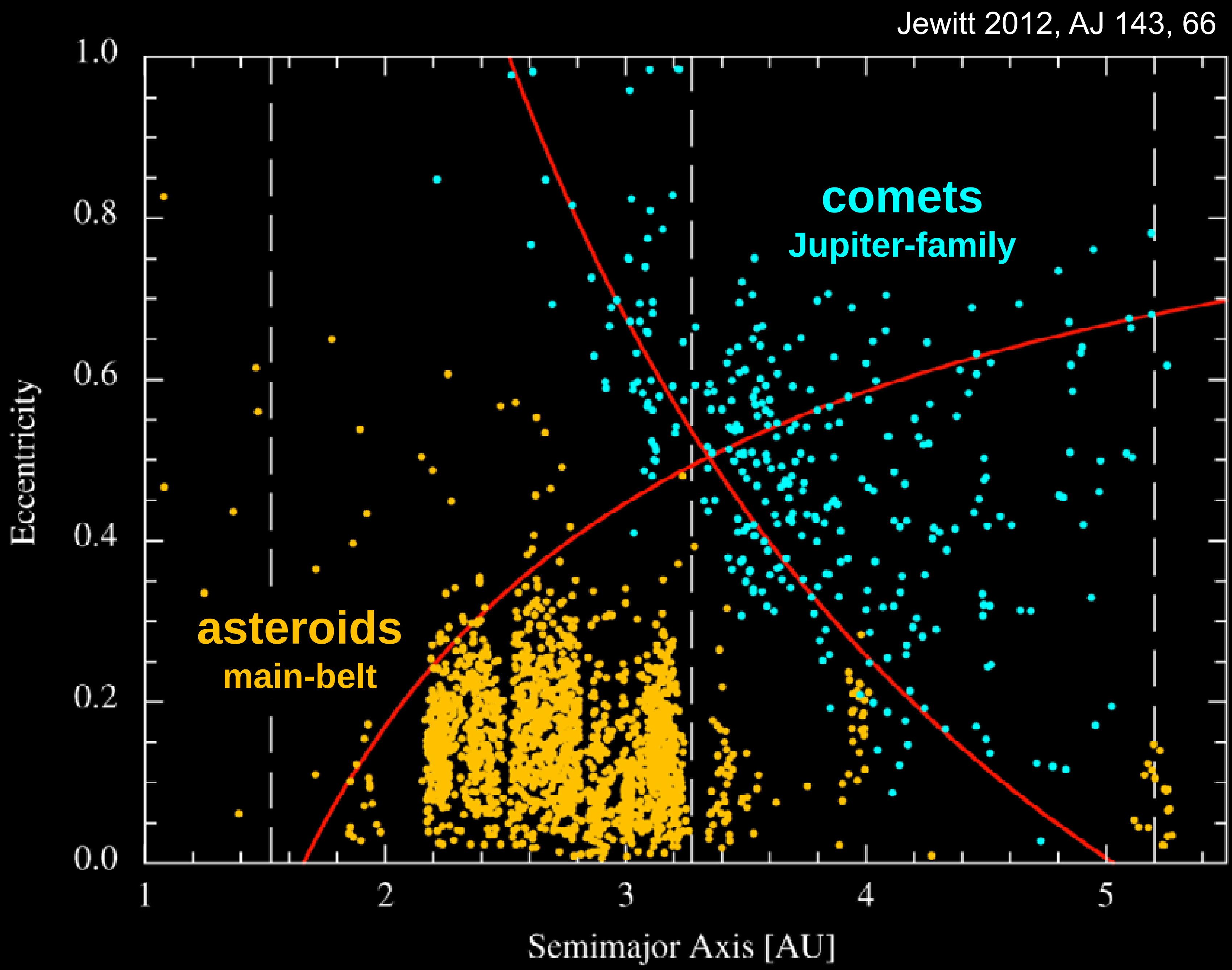

Jewitt 2012, AJ 143, 66
comets
Jupiter-family
asteroids
main-belt
Eccentricity
Semimajor Axis [AU]
1.0
0.8
0.6
0.4
0.2
0.0
1
2
3
4
5

Remote-observation-based classification

observable	**Damocloids ("dead comets")**	
appearance (image)	extended, diffuse	point-source
composition (spectrum)	ice-bearing	not ice-bearing
orbital type	excited (large *a*, *e*, *i*)	stable (small *a*, *e*, *i*)

Remote-observation-based classification

observable	impacted asteroids	
appearance (image)	extended, diffuse	point-source
composition (spectrum)	ice-bearing	not ice-bearing
orbital type	excited (large *a, e, i*)	stable (small *a, e, i*)

P/2010 A2 LINEAR

Jewitt et al. 2010,
Nature 467, 817

596 Scheila

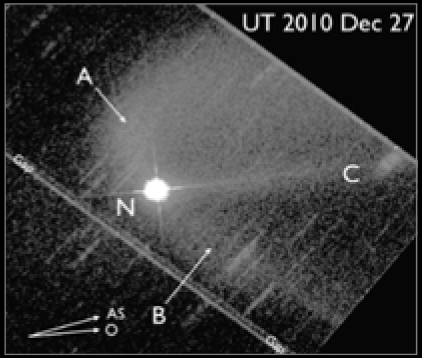

Jewitt et al. 2011,
ApJL 733, L4

P/2012 F5 Gibbs

Stevenson et al. 2012,
ApJ 759, 142

Remote-observation-based classification

observable	main-belt comets	
appearance (image)	extended, diffuse	point-source
composition (spectrum)	ice-bearing	not ice-bearing
orbital type	excited (large *a*, *e*, *i*)	stable (small *a*, *e*, *i*)

133P/Elst-Pizarro Hsieh et al. 2010, MNRAS 408, 363

perihelion 2002 **aphelion 2005** **perihelion 2007**

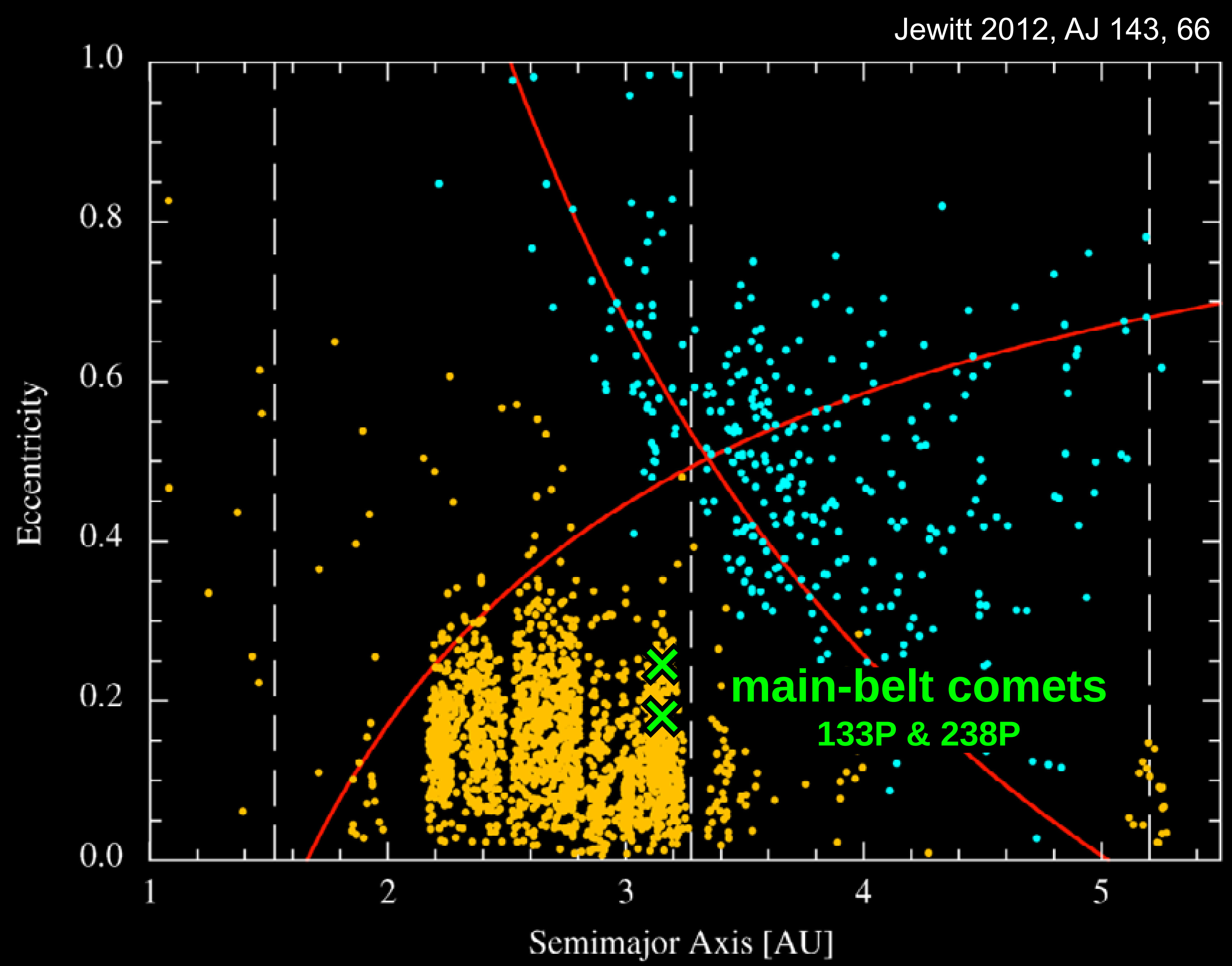

Jewitt 2012, AJ 143, 66
1.0
0.8
0.6
0.4
0.2
0.0
Eccentricity
1
2
3
4
5
Semimajor Axis [AU]
main-belt comets
133P & 238P

The Palomar Transient Factory (PTF) survey

- 60-second exposures
- 1.01-arcsec / pixel resolution
- 7.2 deg^2 mosaic
  (~20% of telescope's focal plane)
- 11 CCDs , 2048 × 4096 each
- filters used:
  Mould-R (600 - 720 nm)
  SDSS-g′ (400 - 550 nm)
- down to $R \approx 20.5$ mag (5-σ)
- 2-arcsec seeing typical
- 5-day cadence : supernova search
- 1-hour cadence : ~2000 deg^2 imaged 2× per night
- Science-data collection started March 2009
- Data processed and archived by
  IPAC (Infrared Processing and
  Analysis Center) @ Caltech

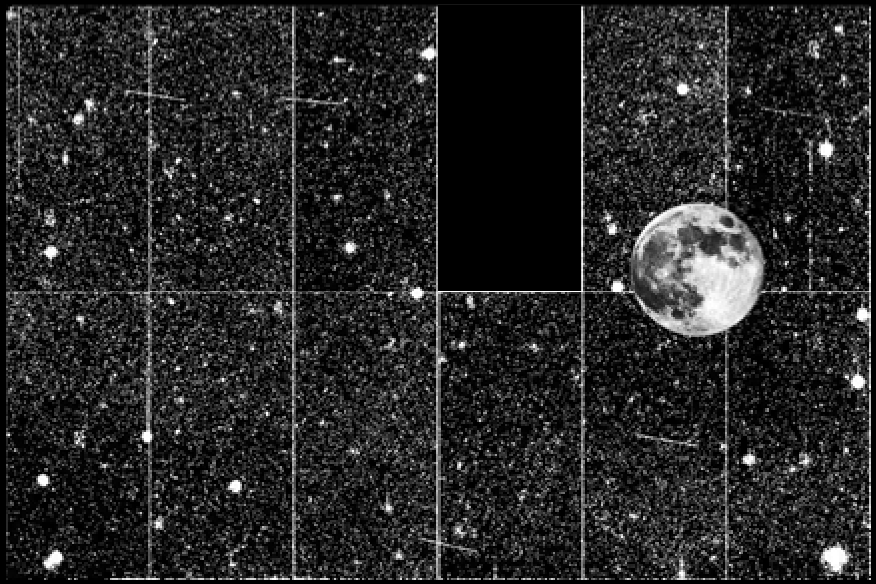

48-inch (1.2-m) Schmidt Telescope

The Palomar Transient Factory (PTF) survey

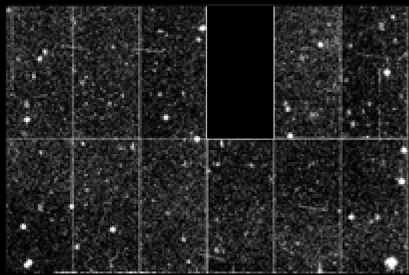

~150,000 images
(~50 TB raw data)

$x_1, y_1, t_1, \ldots$
$x_2, y_2, t_2, \ldots$
$\vdots$

~ 700 million
transient detections

~ 680 million garbage detections

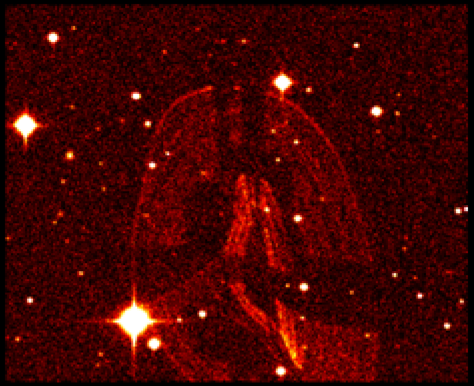

"ghosts"

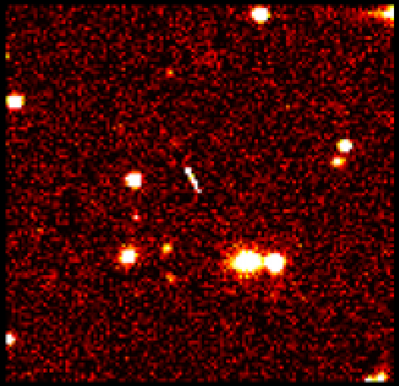

radiation hits

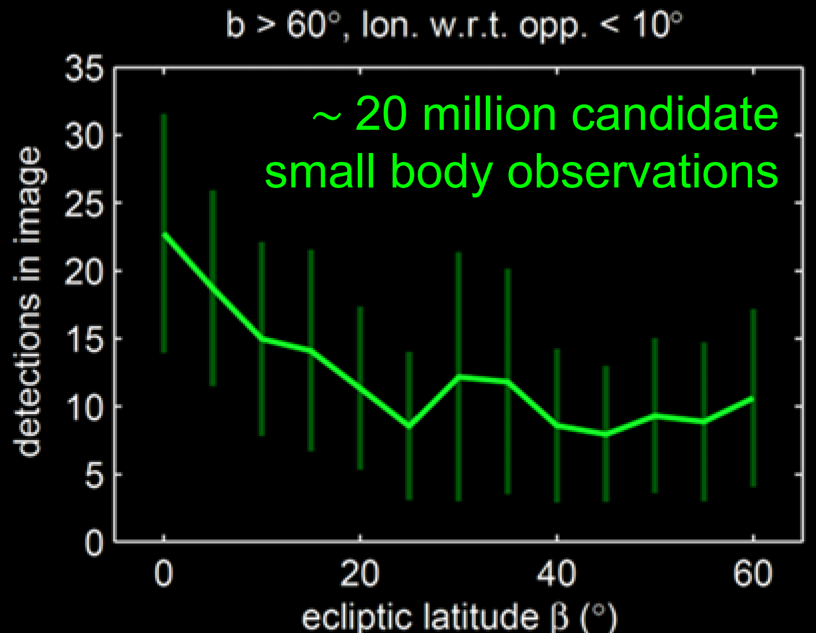

Searching for small bodies with known orbits

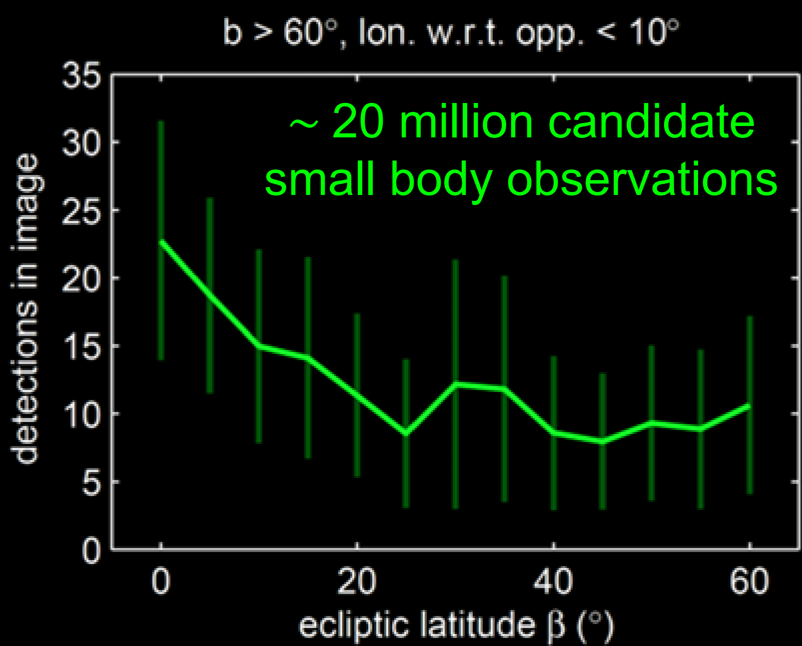

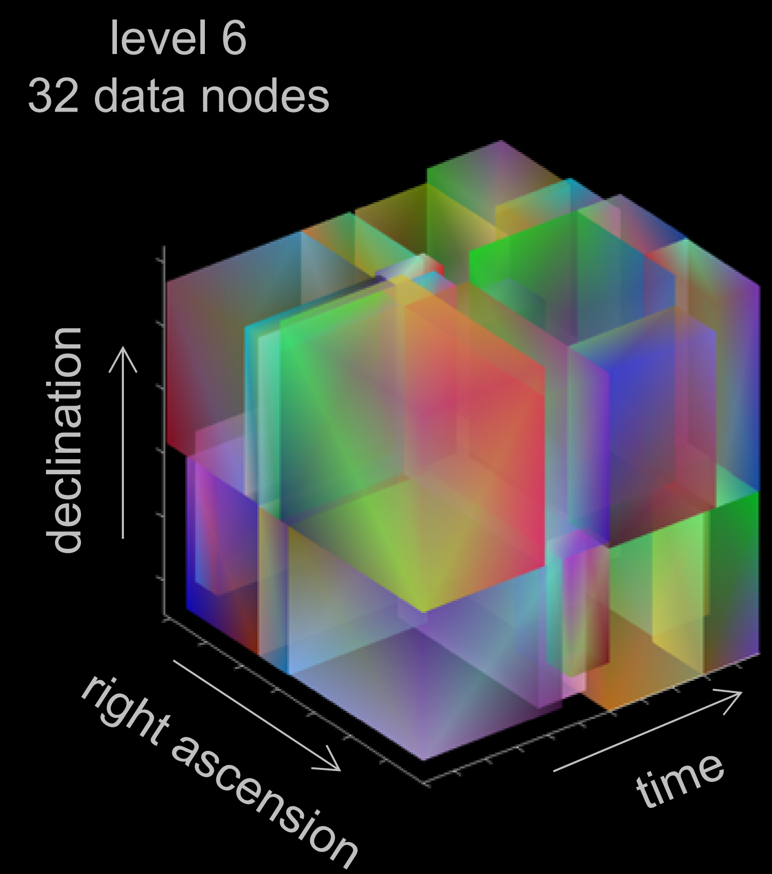

"kd-tree" application to sky surveys:
Kubica et al. 2007, Icarus 189, 151

Searching for small bodies with known orbits

data tree

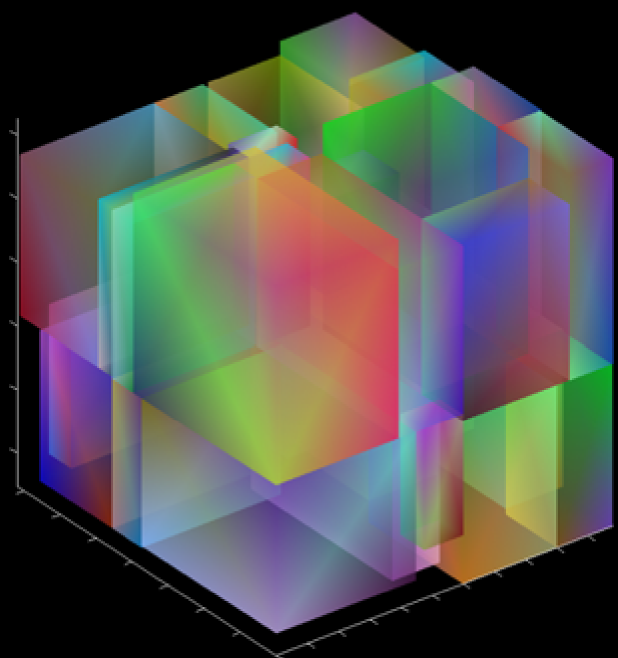

~20 million candidate
small body observations

ephemeris tree

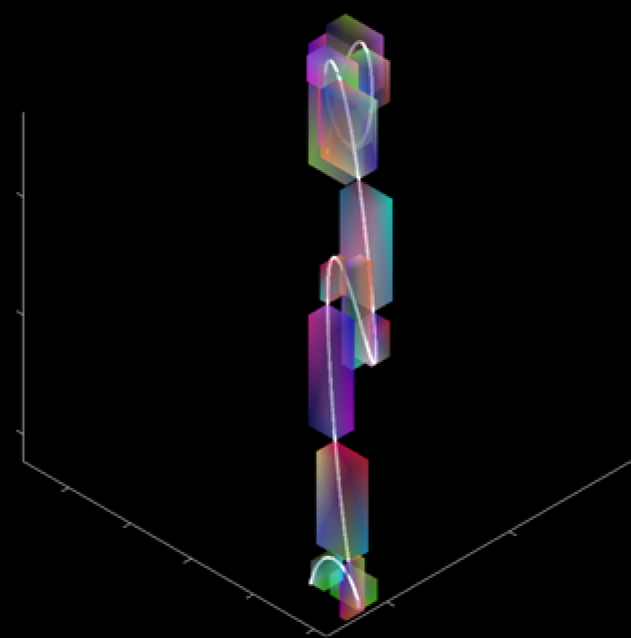

~1000-point (3-year) ephemeris
from JPL's HORIZONS integrator

Summary of observed known small bodies

	main-belt asteroids	Trojans & Hildas	comets	NEOs	TNOs	Centaurs
observations	2,013,279	50,056	1,052	6,586	454	336
unique objects	221,402	5,259	129	1,257	48	27
fraction of known	0.39	0.55	0.06	0.13	0.03	0.13

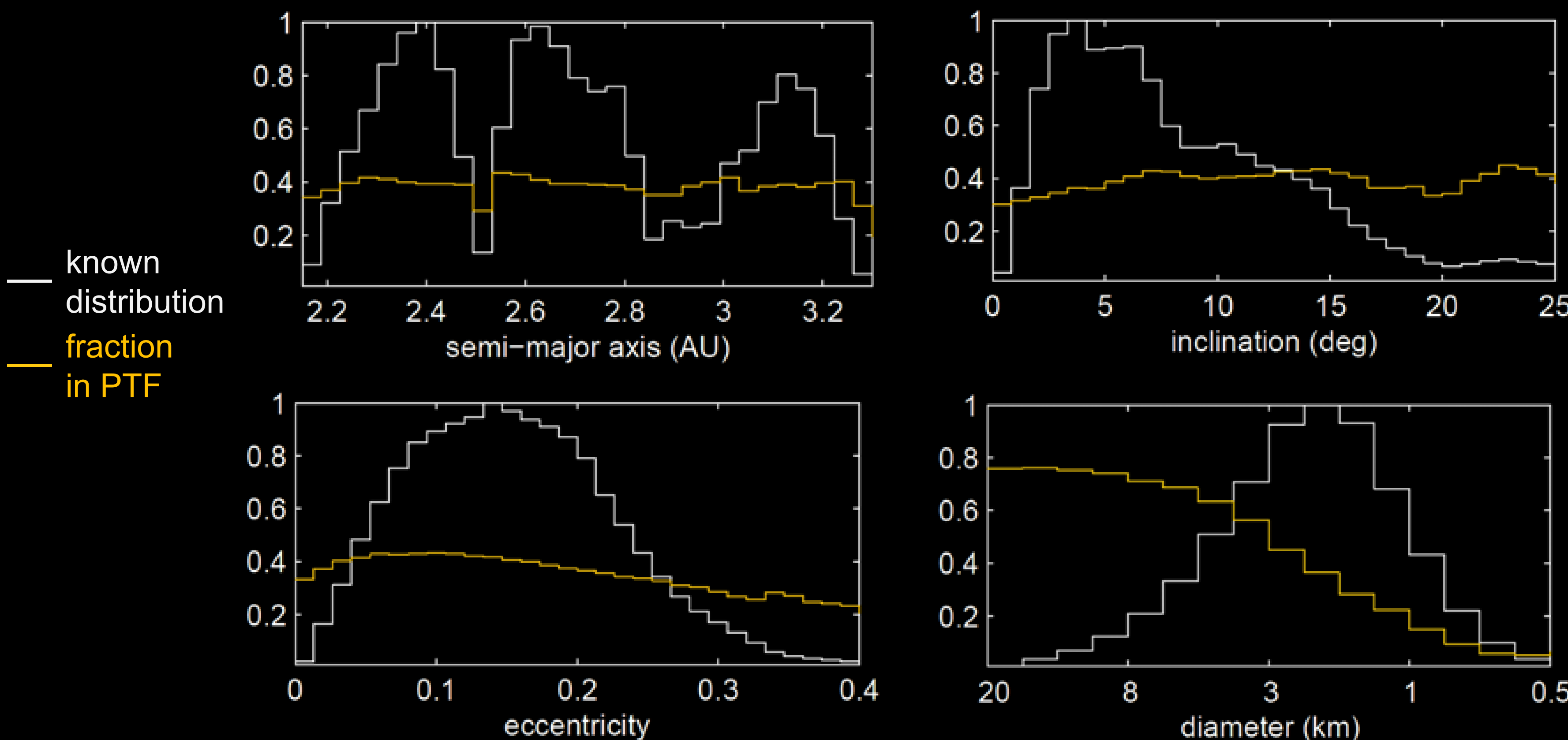

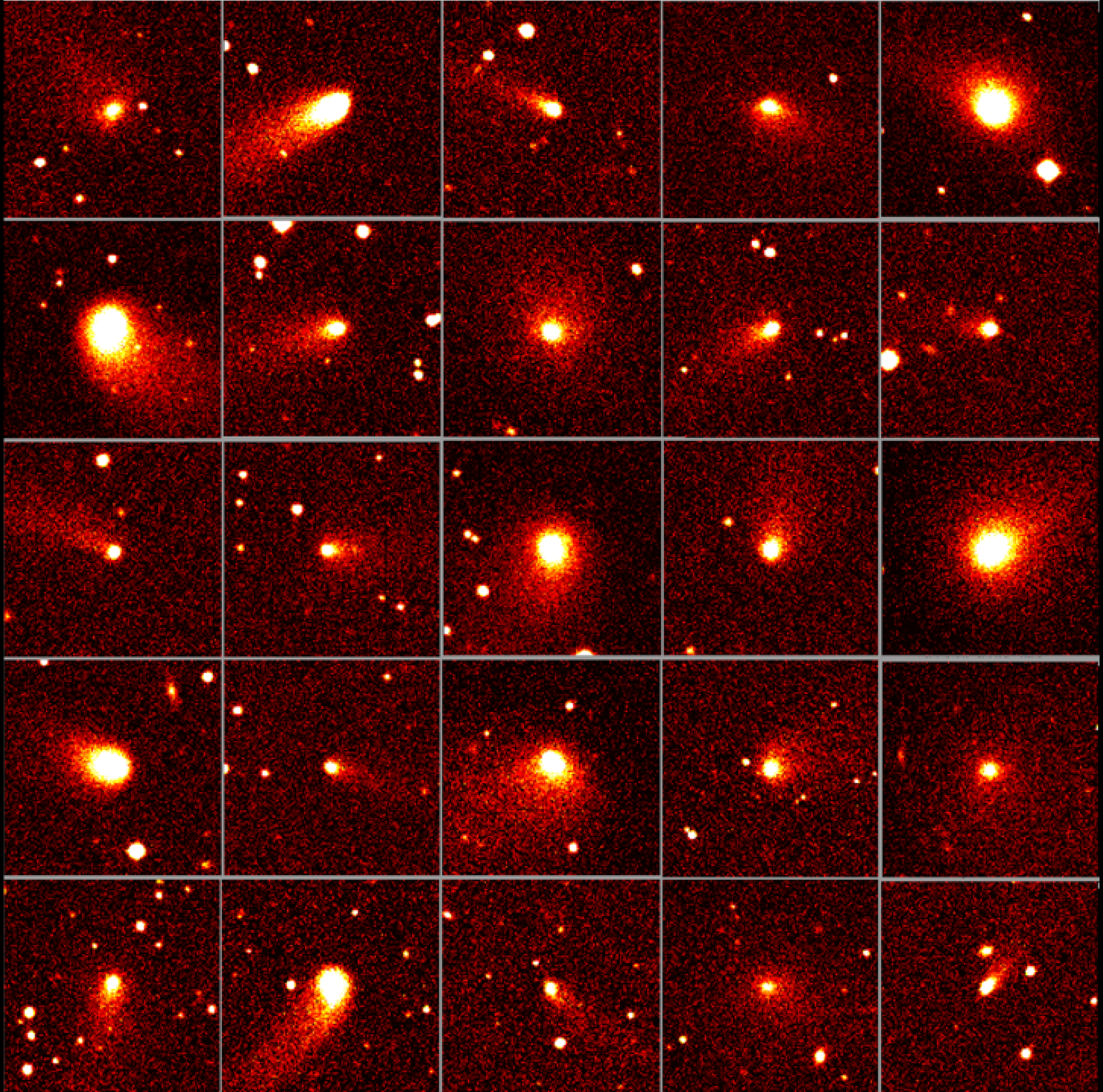

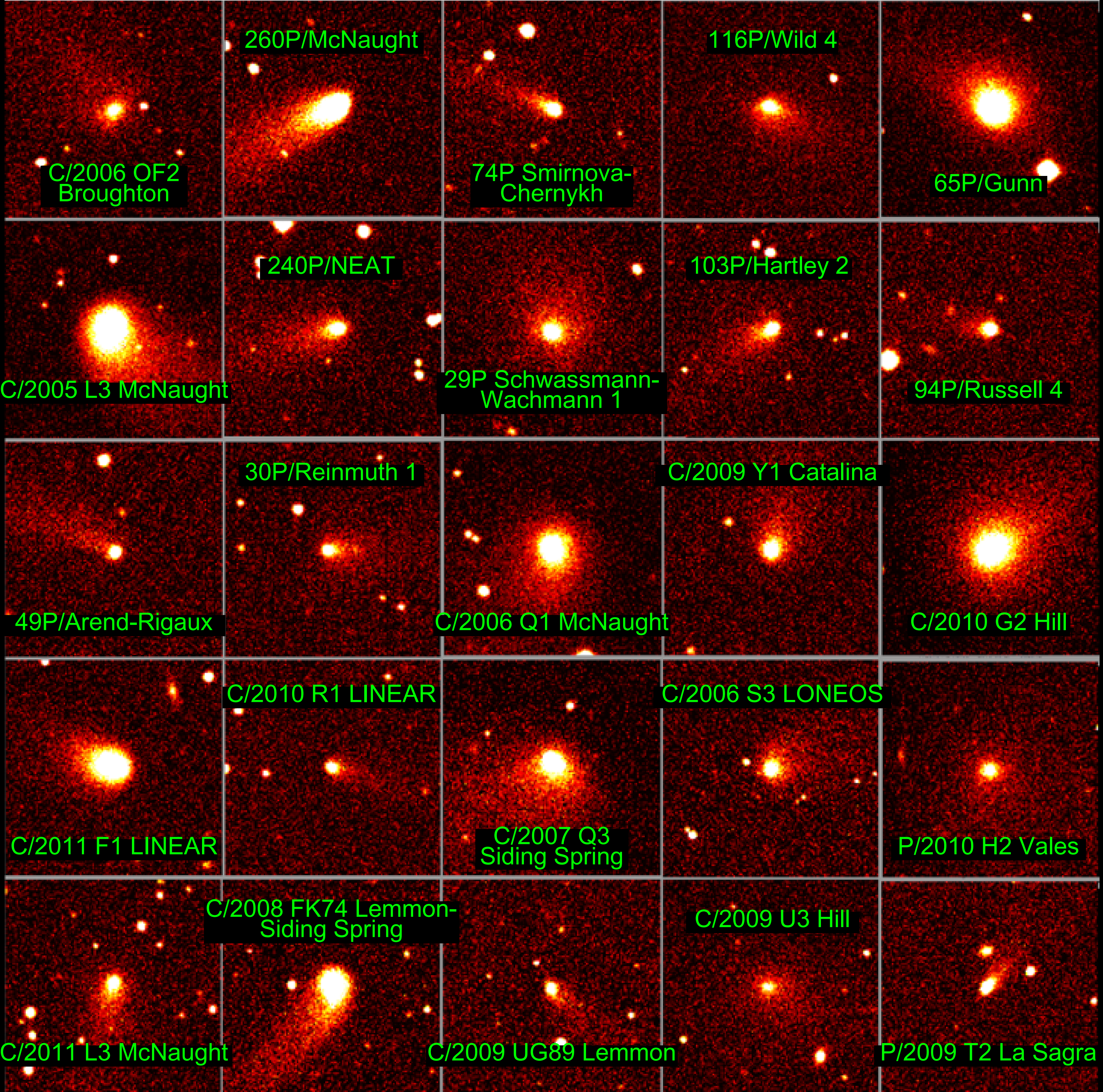
C/2006 OF2 Broughton
260P/McNaught
74P Smirnova-Chernykh
116P/Wild 4
65P/Gunn
C/2005 L3 McNaught
240P/NEAT
29P Schwassmann-Wachmann 1
103P/Hartley 2
94P/Russell 4
49P/Arend-Rigaux
30P/Reinmuth 1
C/2006 Q1 McNaught
C/2009 Y1 Catalina
C/2010 G2 Hill
C/2011 F1 LINEAR
C/2010 R1 LINEAR
C/2007 Q3 Siding Spring
C/2006 S3 LONEOS
P/2010 H2 Vales
C/2011 L3 McNaught
C/2008 FK74 Lemmon-Siding Spring
C/2009 UG89 Lemmon
C/2009 U3 Hill
P/2009 T2 La Sagra

A rich small body dataset in PTF

High cadence lightcurves ⟹ object spin rate, shape, binarity

Pilot study based on Feb-2010 imagery of the M44 field:
Polishook et al. 2012, Asteroid rotation periods from PTF, MNRAS 421, 2094

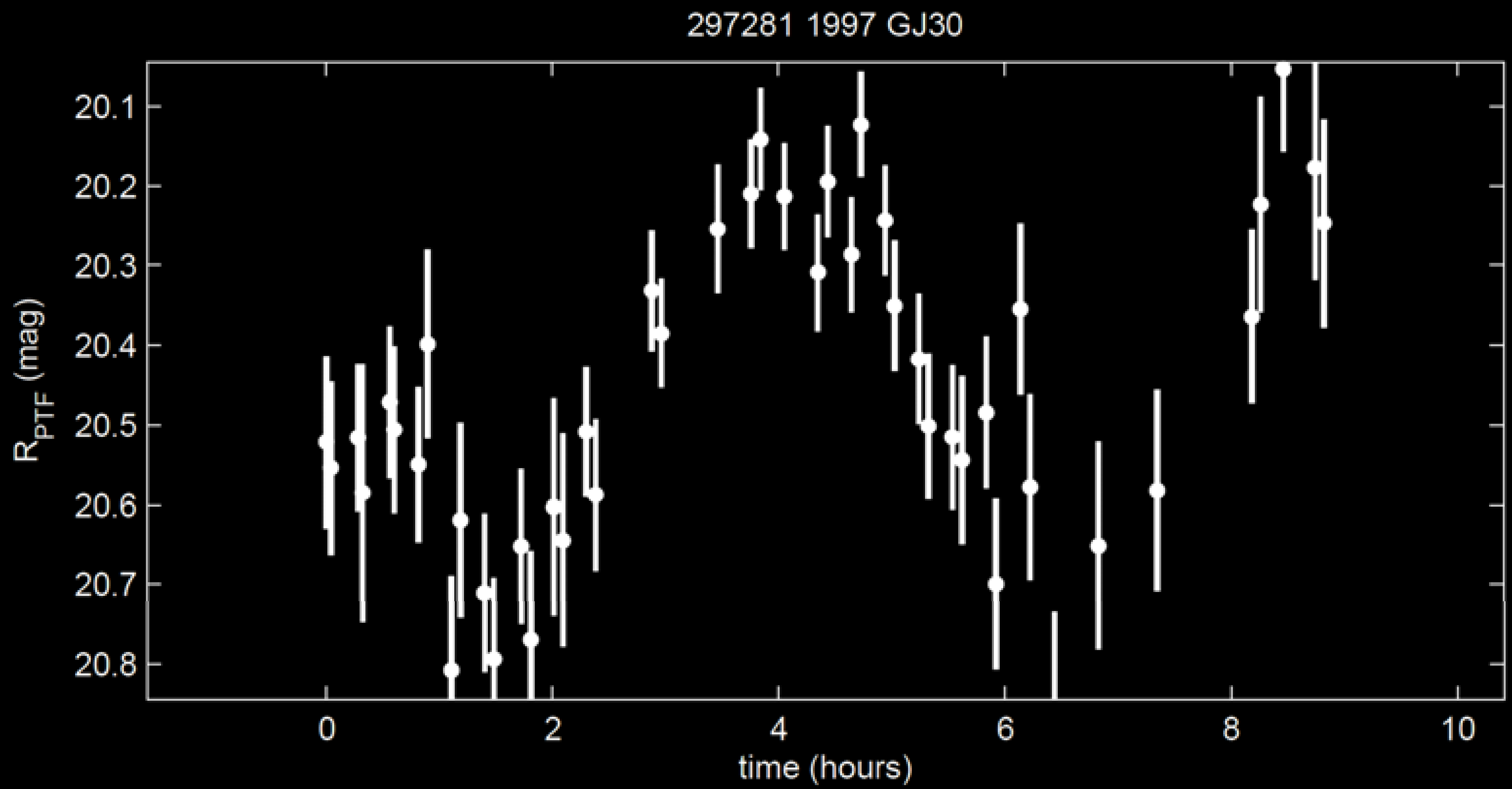

2048 known objects in PTF have ≥ 20 observations/night on at least one night

A rich small body dataset in PTF

High cadence lightcurves $\Longrightarrow$ object spin rate, shape, binarity

Pilot study based on Feb-2010 imagery of the M44 field:
Polishook et al. 2012, Asteroid rotation periods from PTF, MNRAS 421, 2094

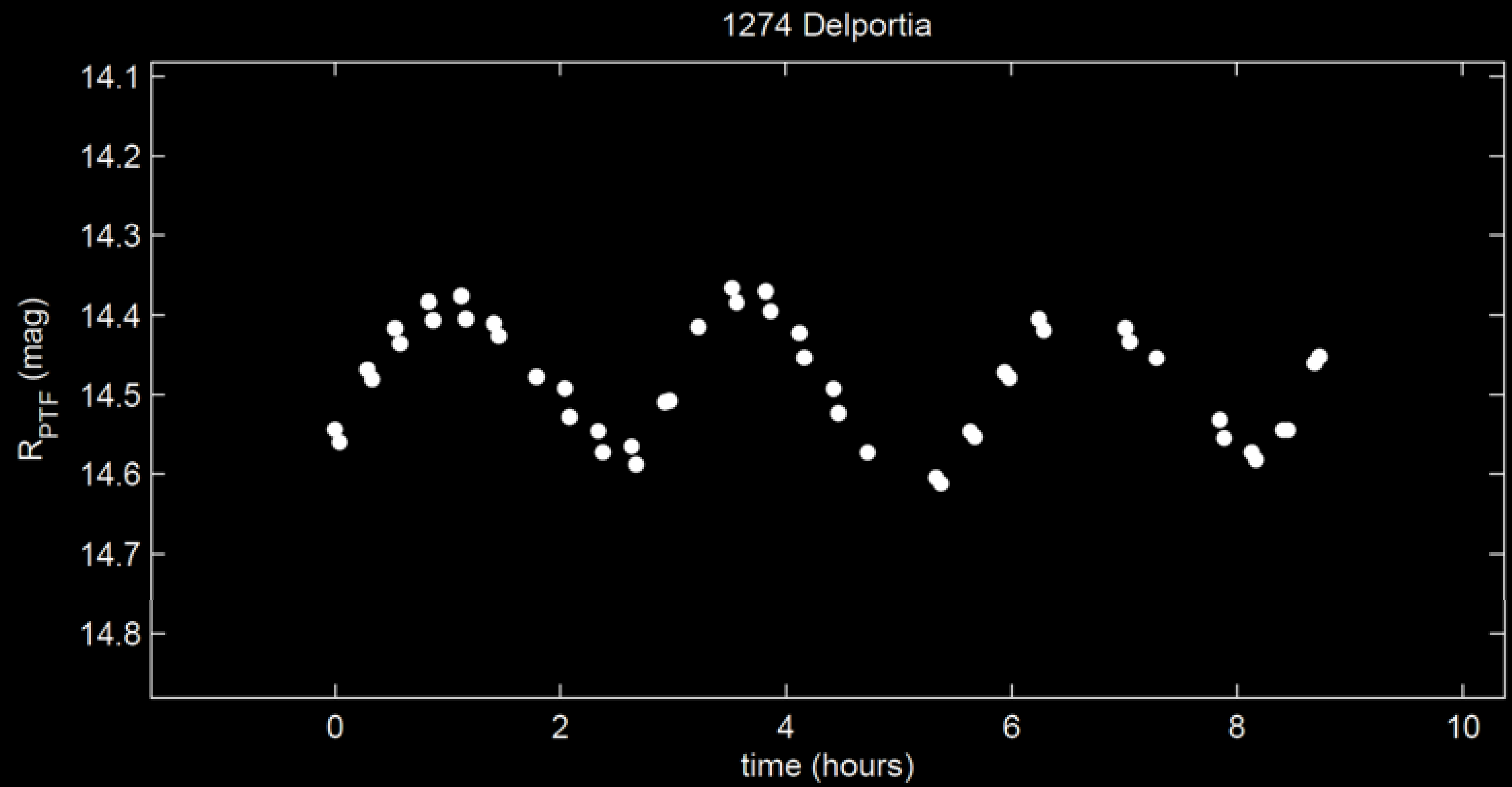

2048 known objects in PTF have ≥ 20 observations/night on at least one night

A rich small body dataset in PTF

High cadence lightcurves ⟹ object spin rate, shape, binarity

Pilot study based on Feb-2010 imagery of the M44 field:
Polishook et al. 2012, Asteroid rotation periods from PTF, MNRAS 421, 2094

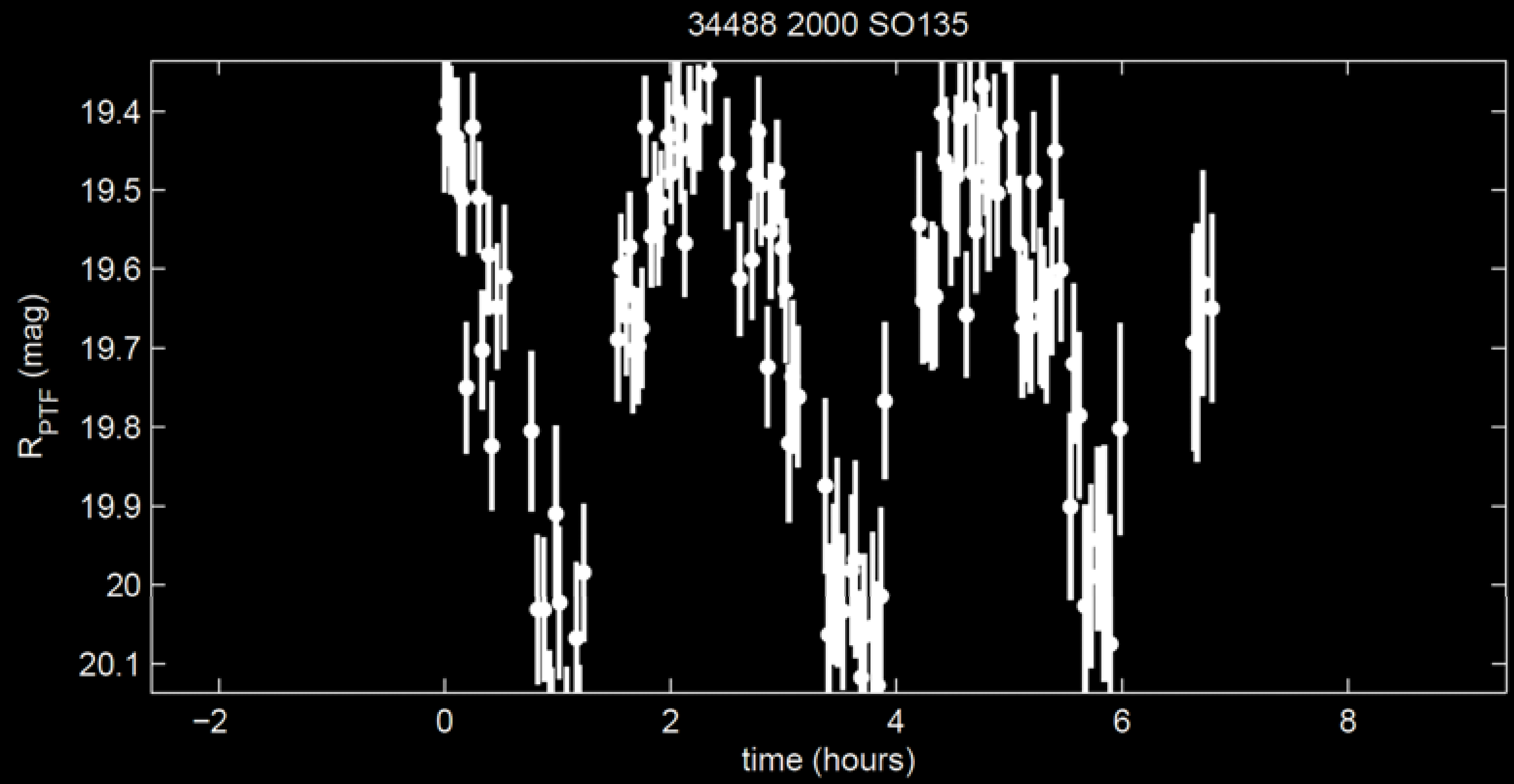

2048 known objects in PTF have ≥ 20 observations/night on at least one night

A rich small body dataset in PTF

High cadence lightcurves ⟹ object spin rate, shape, binarity

Pilot study based on Feb-2010 imagery of the M44 field:
Polishook et al. 2012, Asteroid rotation periods from PTF, MNRAS 421, 2094

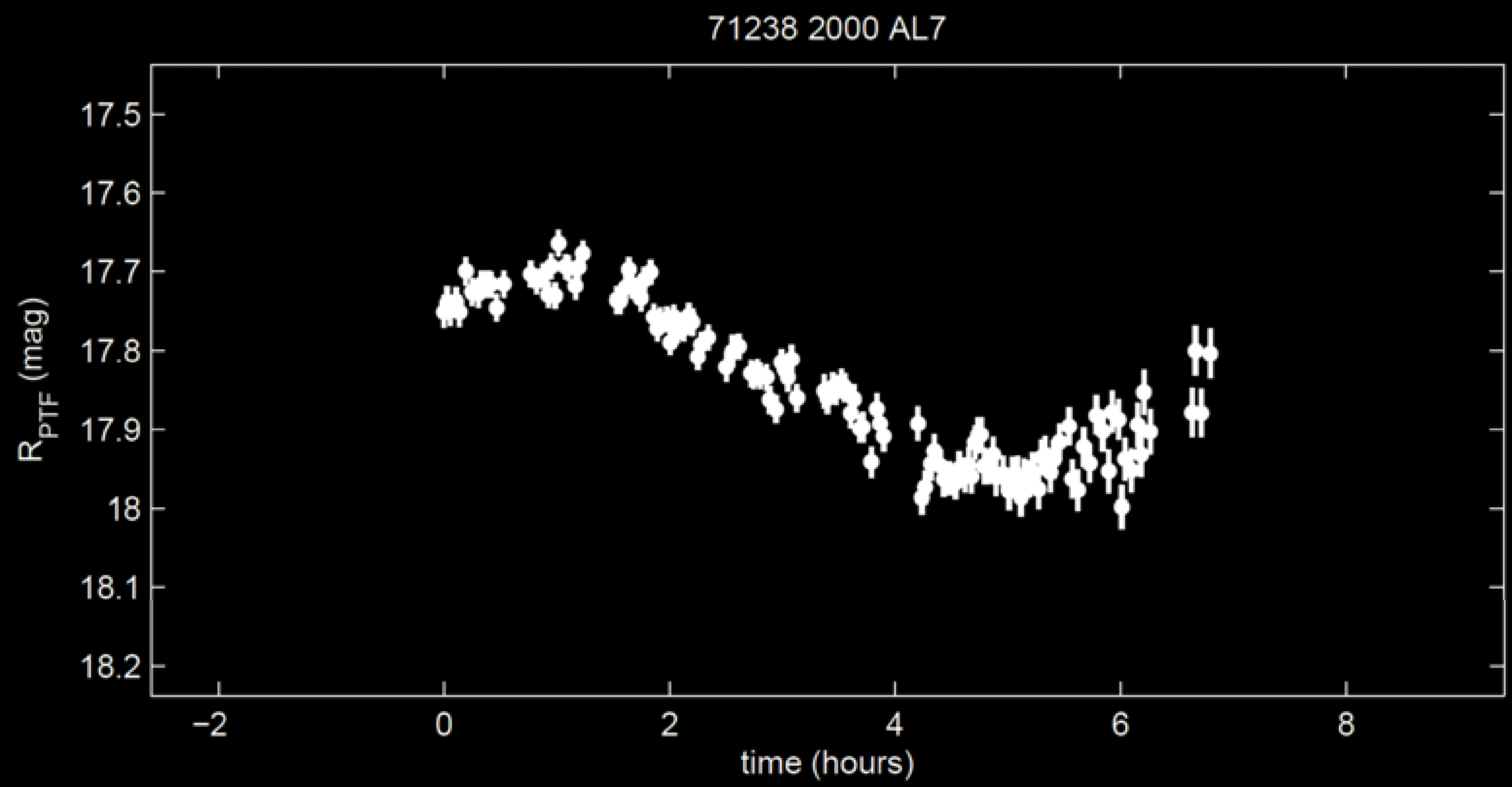

2048 known objects in PTF have ≥ 20 observations/night on at least one night

A rich small body dataset in PTF

High cadence lightcurves ⟹ object spin rate, shape, binarity

Pilot study based on Feb-2010 imagery of the M44 field:
Polishook et al. 2012, Asteroid rotation periods from PTF, MNRAS 421, 2094

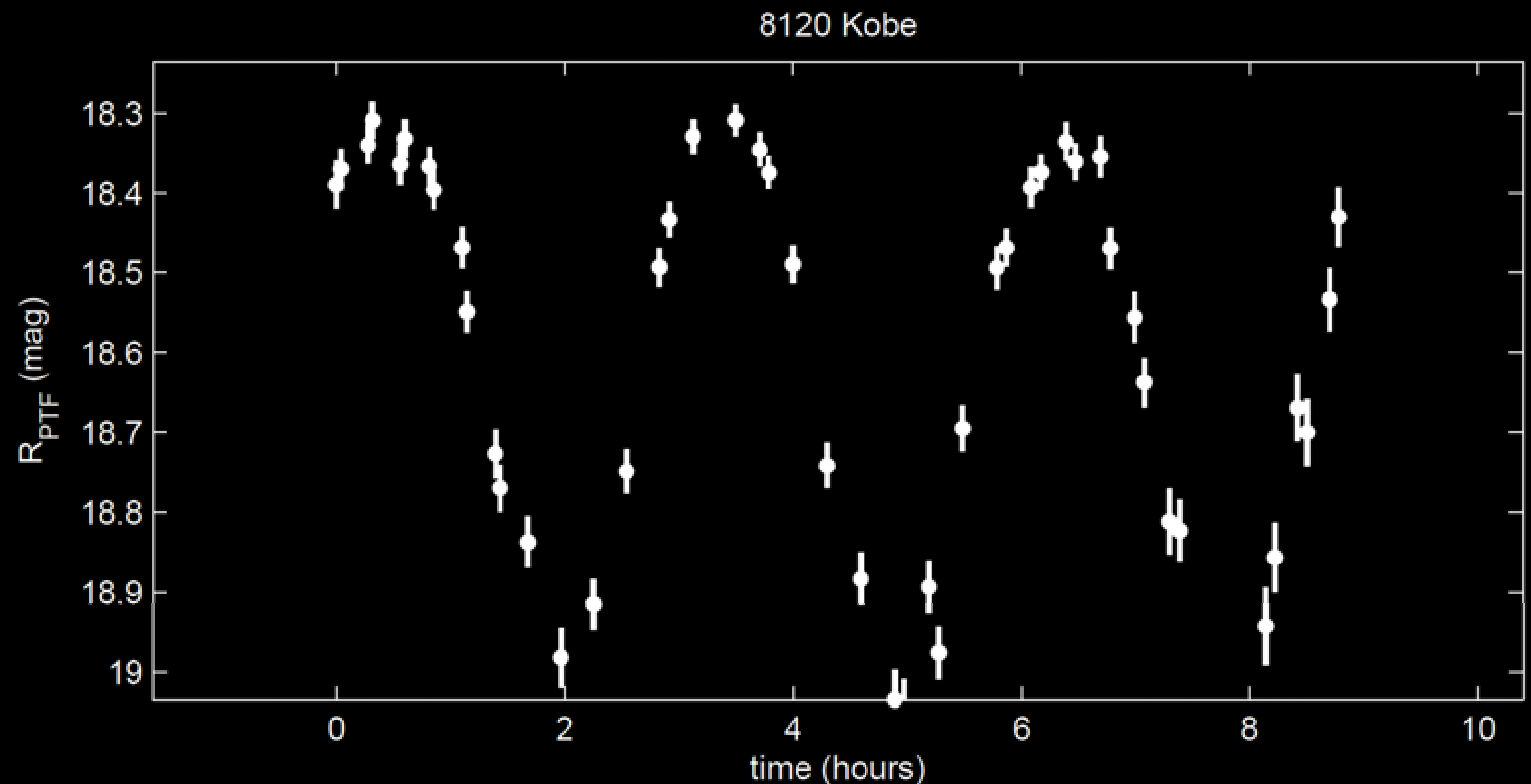

2048 known objects in PTF have ≥ 20 observations/night on at least one night

A rich small body dataset in PTF

Distance-corrected magnitude depends on phase-angle (Sun-asteroid-Earth) and the following physical/surface properties (Hapke model)

- grain size
- grain scattering function
- grain porosity
- shadowing & coherent backscatter
- mean topographic slope
- mean object diameter

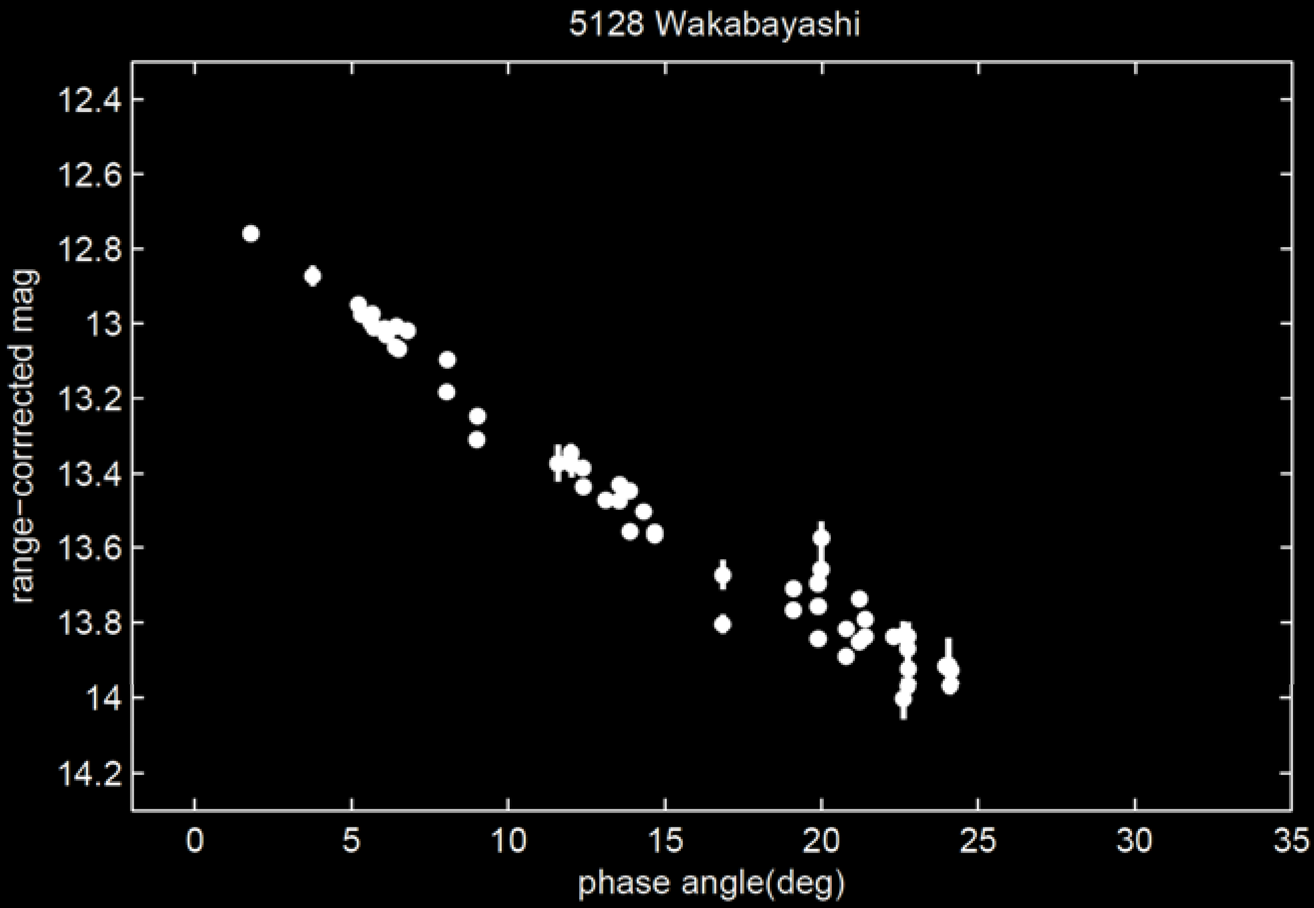

1845 known objects in PTF have observations in ≥ 7 phase-angle bins 3° wide, including 0° to 3°

A rich small body dataset in PTF

Distance-corrected magnitude depends on phase-angle (Sun-asteroid-Earth) and the following physical/surface properties (Hapke model)

- grain size
- grain scattering function
- grain porosity
- shadowing & coherent backscatter
- mean topographic slope
- mean object diameter

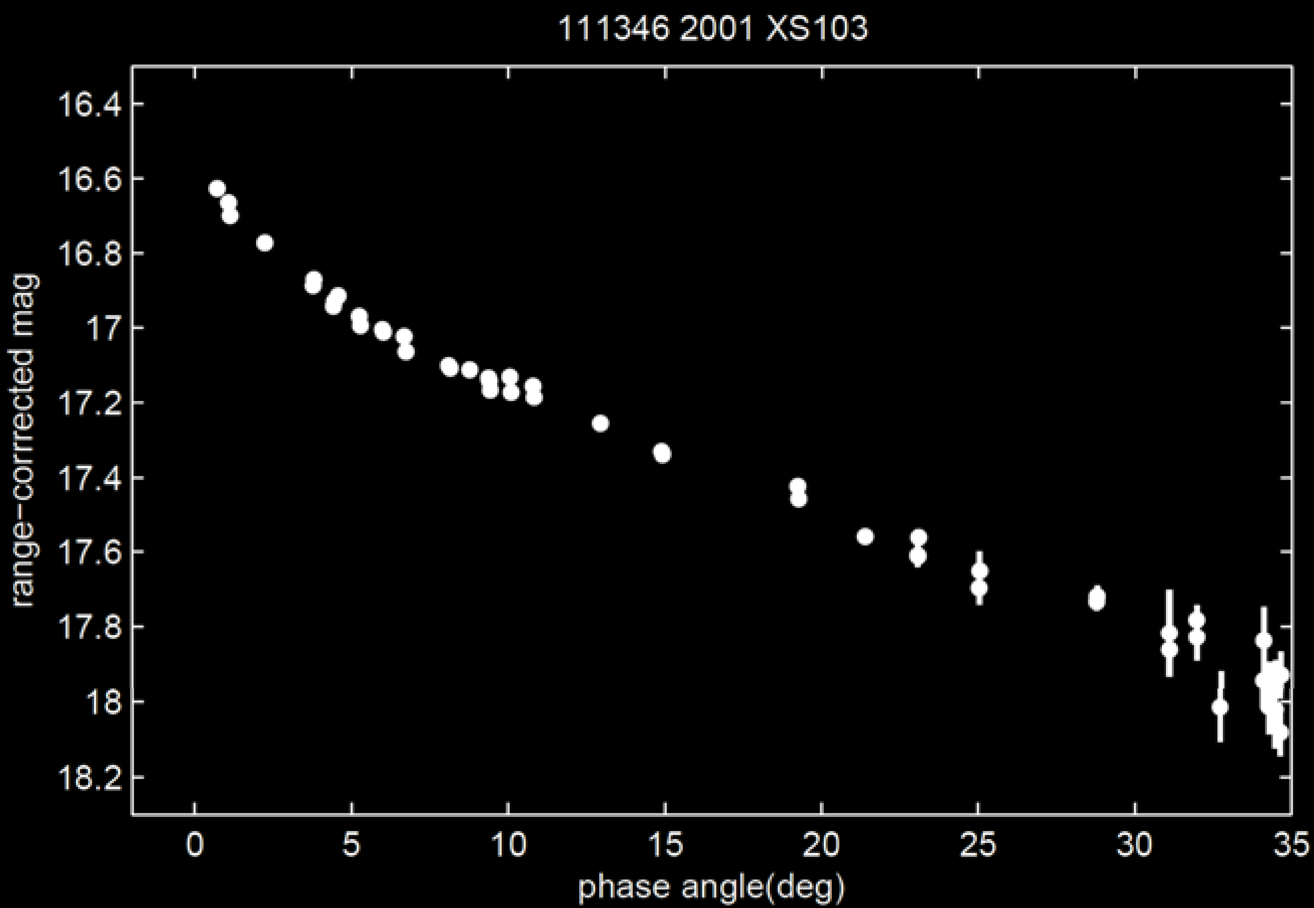

1845 known objects in PTF have observations in ≥ 7 phase-angle bins 3° wide, including 0° to 3°

A rich small body dataset in PTF

Distance-corrected magnitude depends on phase-angle (Sun-asteroid-Earth) and the following physical/surface properties (Hapke model)

- grain size
- grain scattering function
- grain porosity
- shadowing & coherent backscatter
- mean topographic slope
- mean object diameter

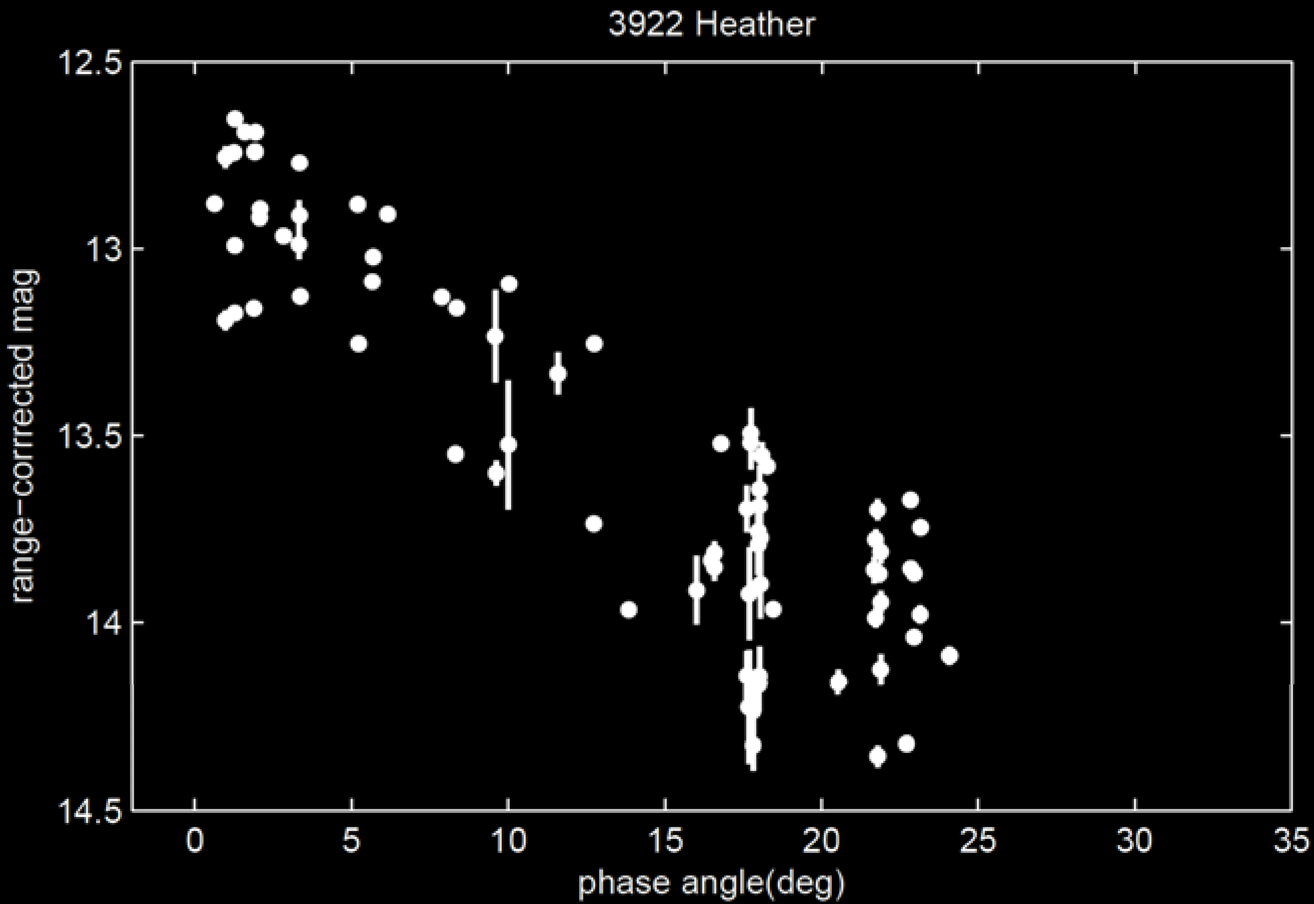

1845 known objects in PTF have observations in ≥ 7 phase-angle bins 3° wide, including 0° to 3°

A rich small body dataset in PTF

Distance-corrected magnitude depends on phase-angle (Sun-asteroid-Earth) and the following physical/surface properties (Hapke model)

- grain size
- grain scattering function
- grain porosity
- shadowing & coherent backscatter
- mean topographic slope
- mean object diameter

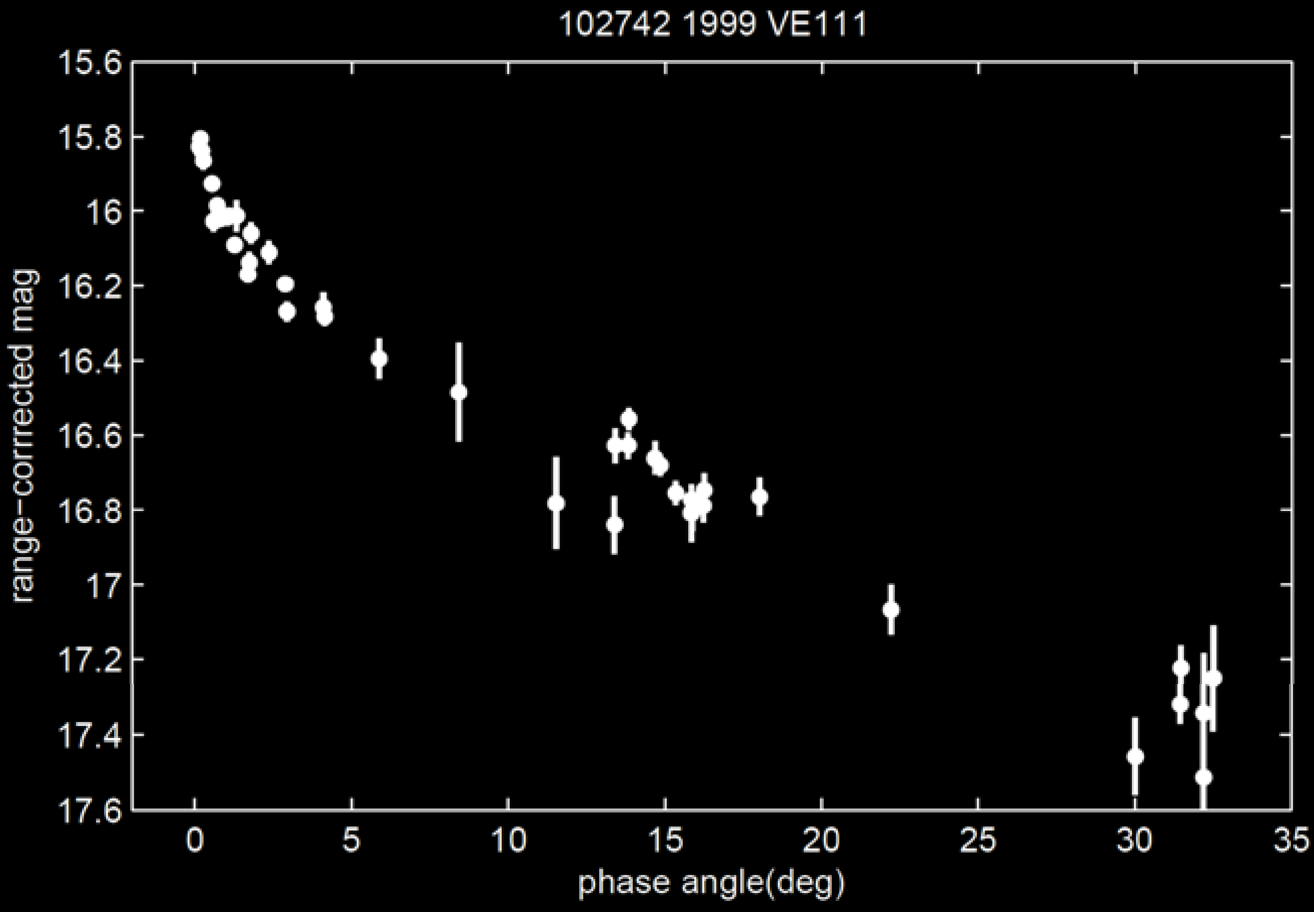

1845 known objects in PTF have observations in ≥ 7 phase-angle bins 3° wide, including 0° to 3°

Summary of observed known small bodies

	main-belt asteroids	Trojans & Hildas	comets	NEOs	TNOs	Centaurs
observations	2,013,279	50,056	1,052	6,586	454	336
unique objects	221,402	5,259	129	1,257	48	27
fraction of known	0.39	0.55	0.06	0.13	0.03	0.13

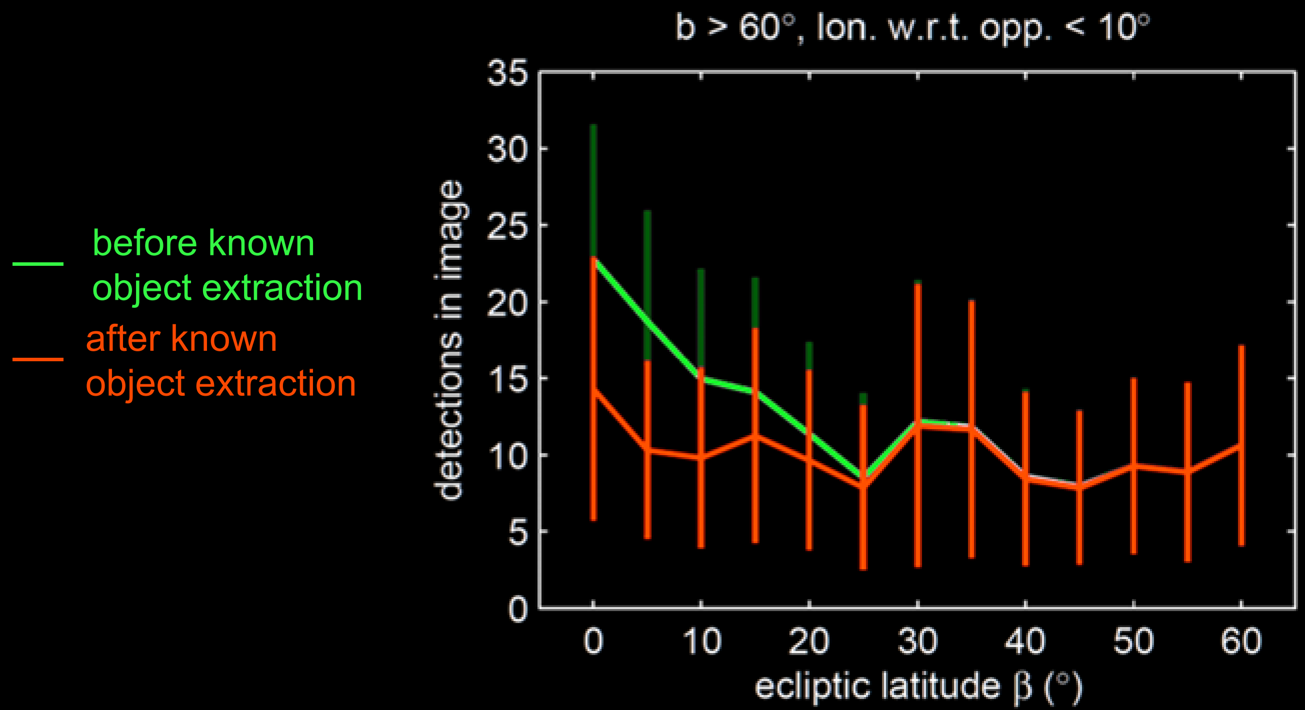

Summary of observed known small bodies

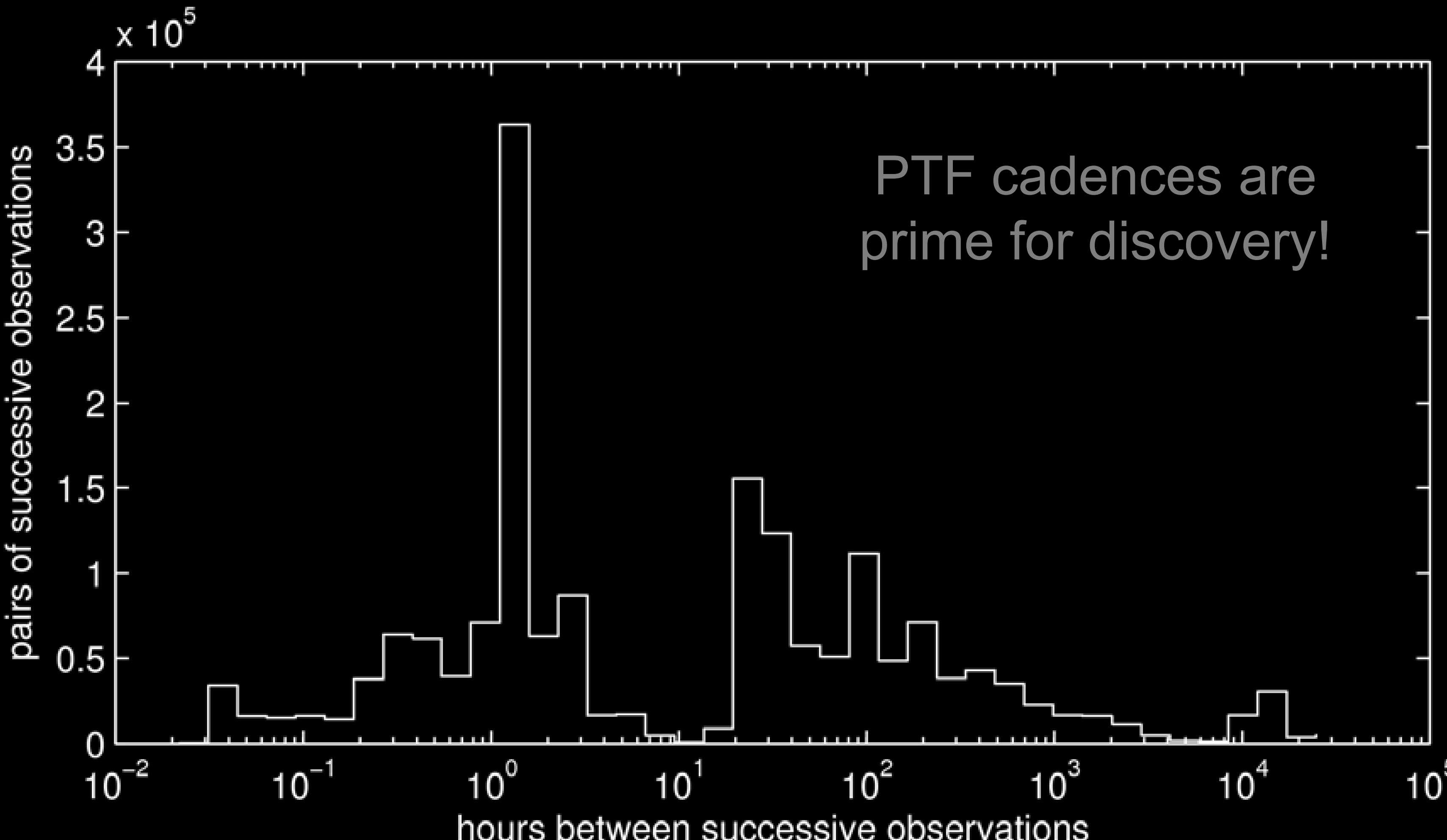

Discovering new small bodies

- kd-tree-based algorithm ran on residual ~18 million detections
- searched for ≥ 3 points (of constant velocity-spacing) spanning ≤ 48 hours
- speed range of 0.01 to 1 arcsec/minute targets main-belt, excluded near-Earth and trans-Neptunian objects
- Manual screening rapidly eliminates the ≥ 95% false-positives
- 1500+ newly-designated multi-night objects confirmed by the Minor Planet Center, including 3 new comets

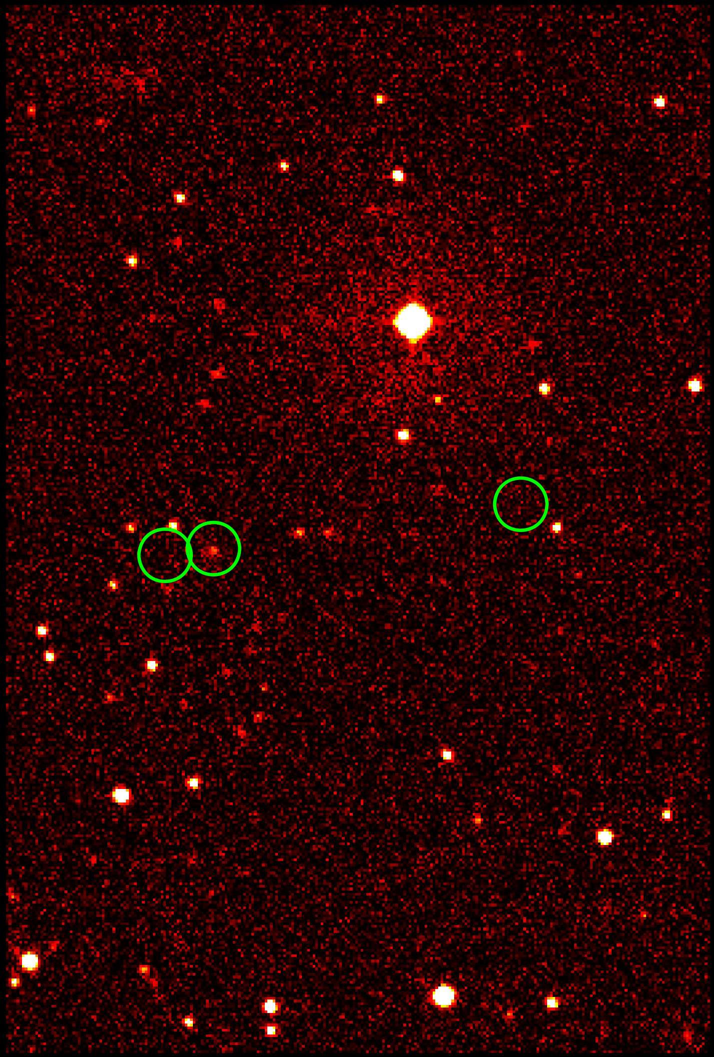

comet 2009 KF37 discovered in PTF

A metric for extendedness

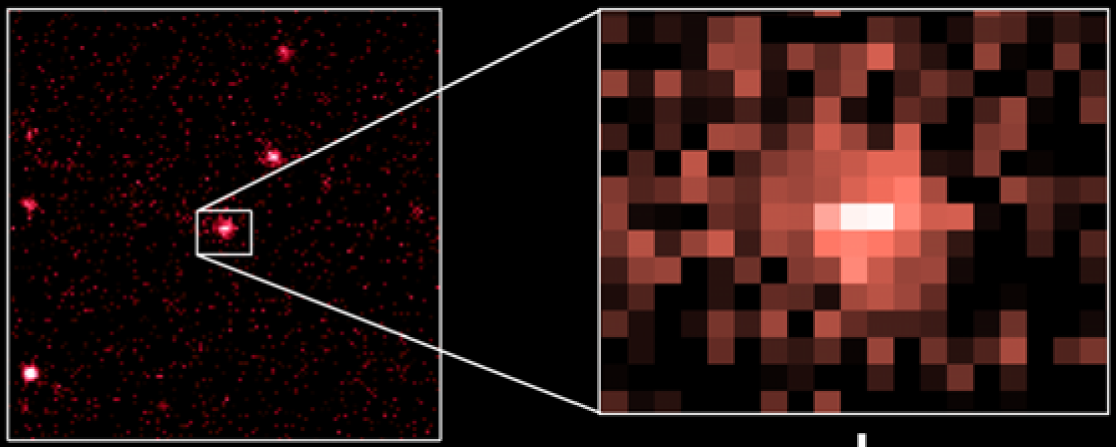

$$\lambda \equiv \frac{\text{total object flux}}{\text{brightest pixel flux}}$$

$$\mu \equiv \log(\lambda_{\text{object}}) - \log(\lambda_{\text{stars}})$$

$\mu > 0 \implies$ extended

$\mu < 0 \implies$ concentrated

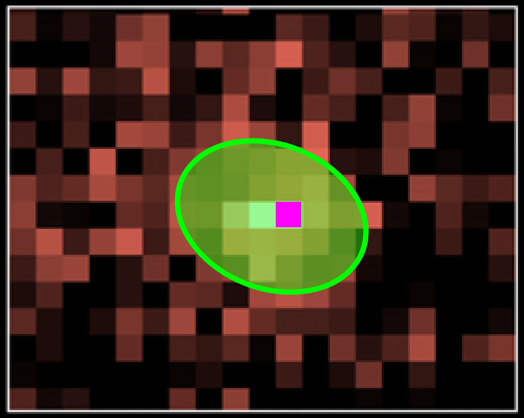

Systematic (non-cometary) extendedness

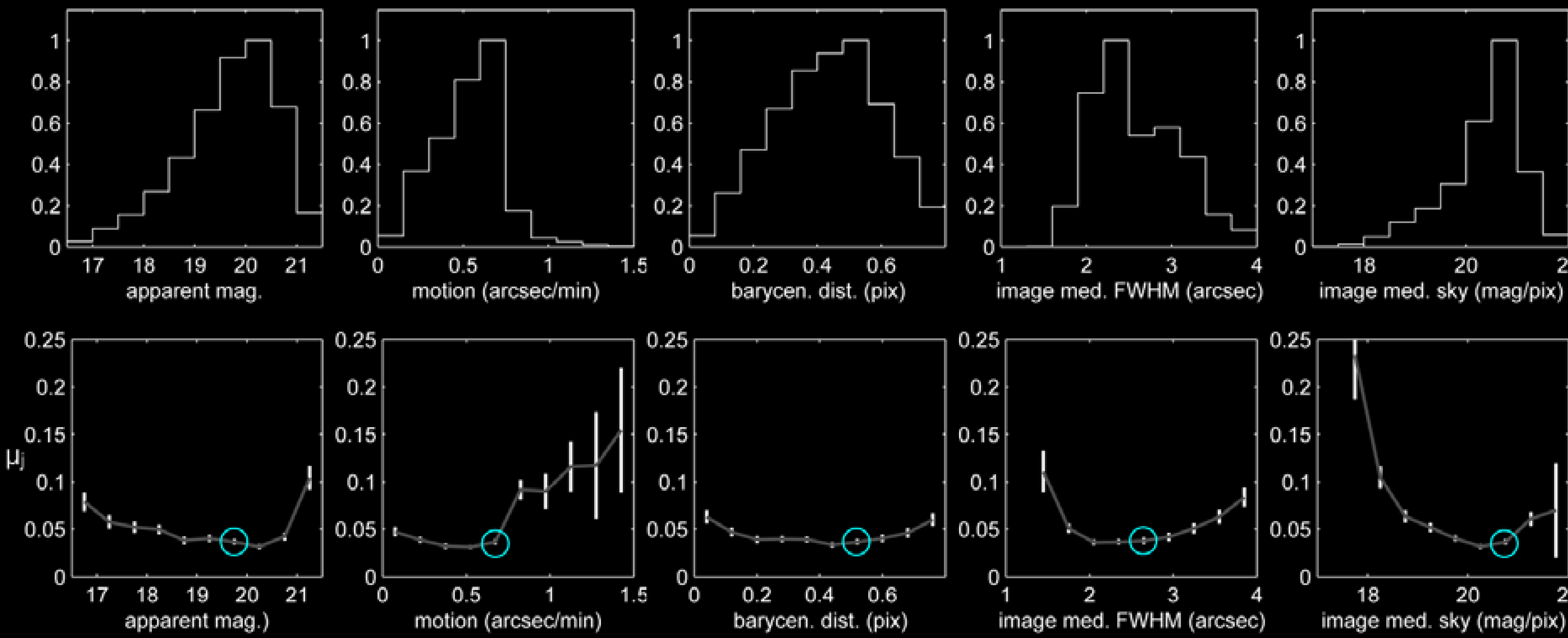

$$\delta\mu \equiv \mu - \mu_j$$

$$\sigma \equiv \sqrt{\sigma_\mu^2 + \sigma_j^2}$$

$$\overline{\delta\mu} \equiv \sum \frac{\delta\mu}{\sigma^2} \qquad \langle\delta\mu\rangle \equiv \left(\sum \frac{1}{\sigma^2}\right)^{-\frac{1}{2}}$$

Quantifying a “cometary” appearance

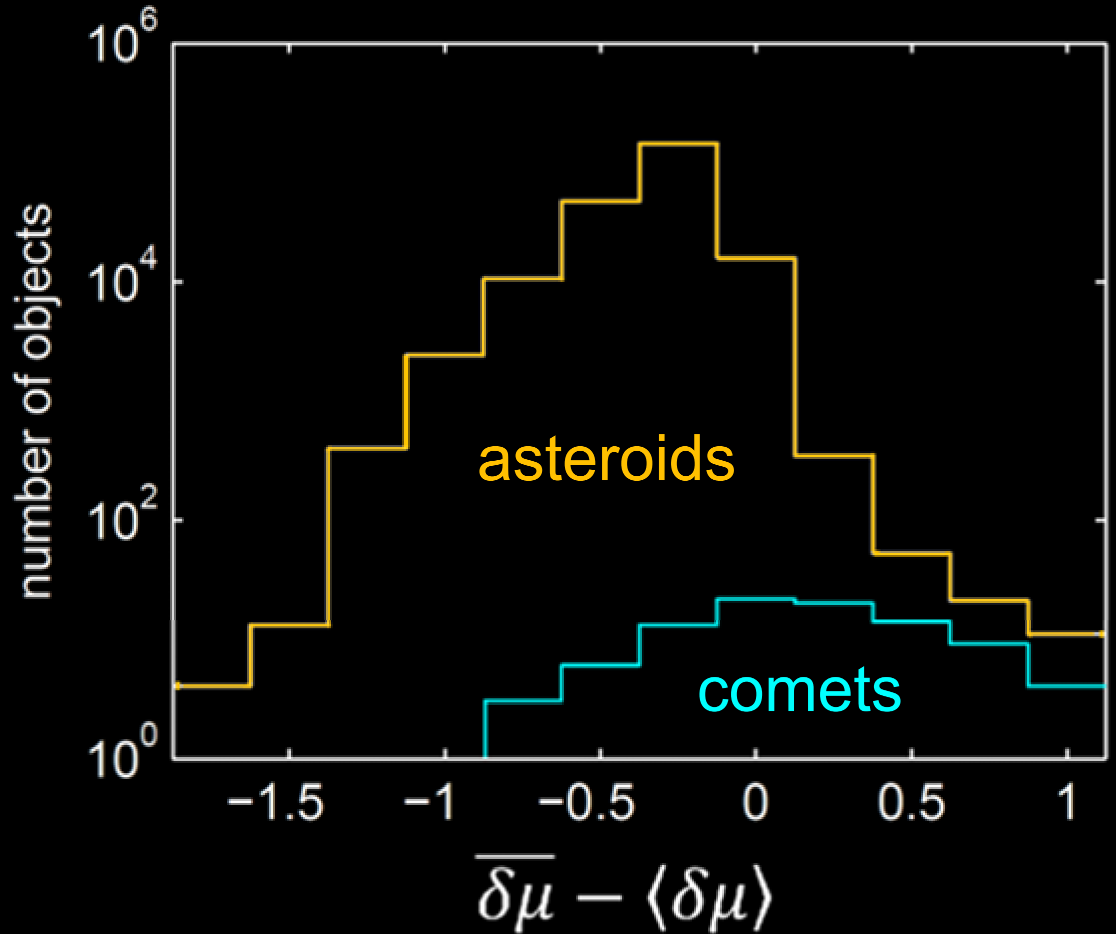

Quantifying a “cometary” appearance

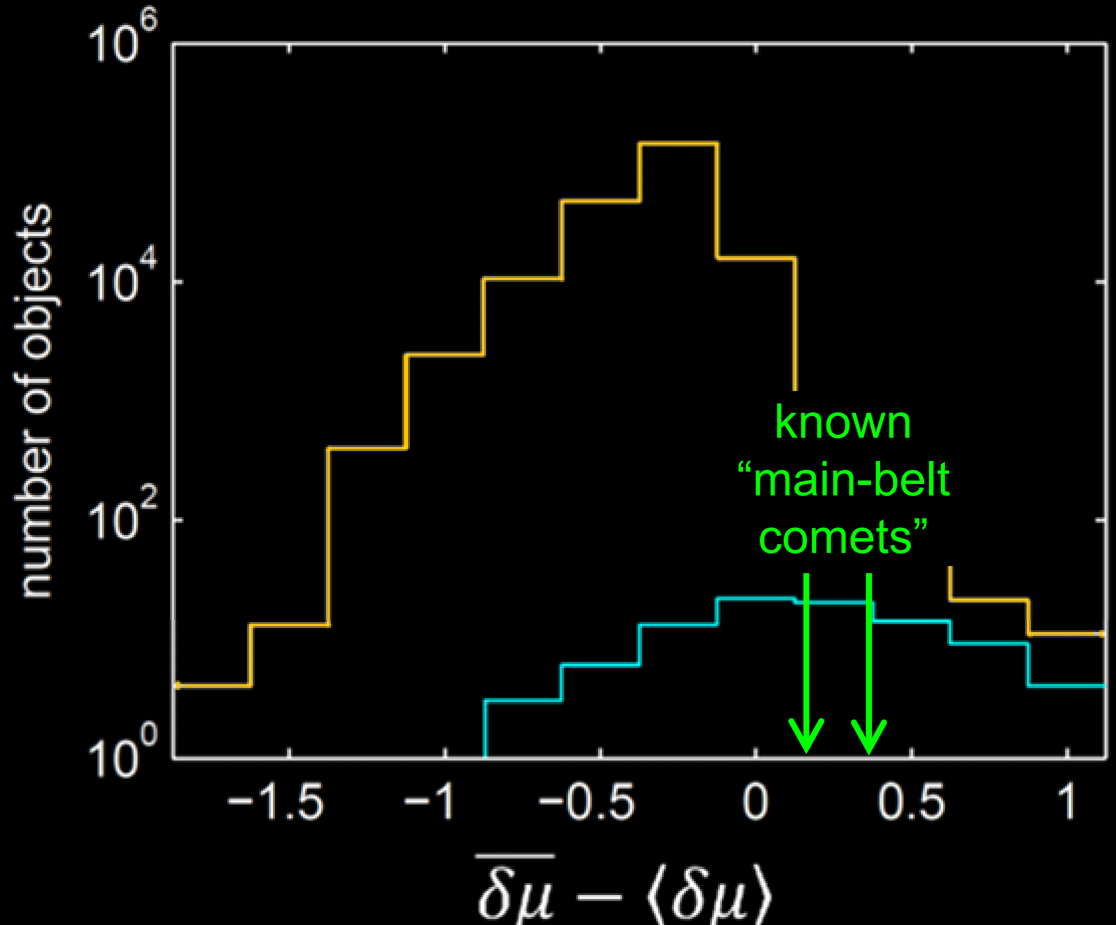

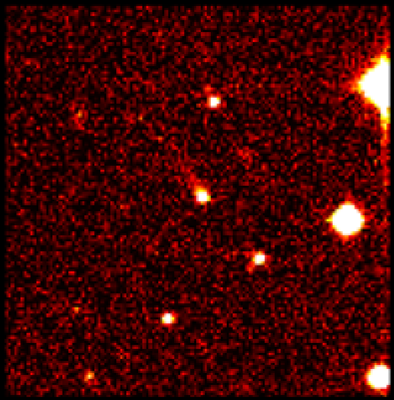

P/2010 R2
La Sagra

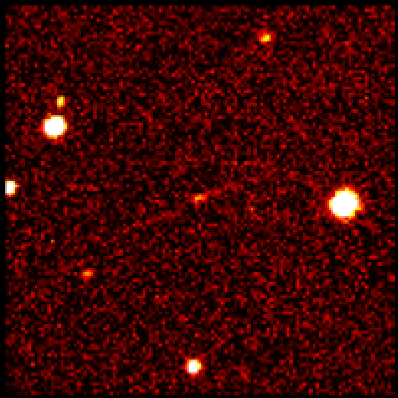

P/2006 VW139
Spacewatch

Quantifying a “cometary” appearance

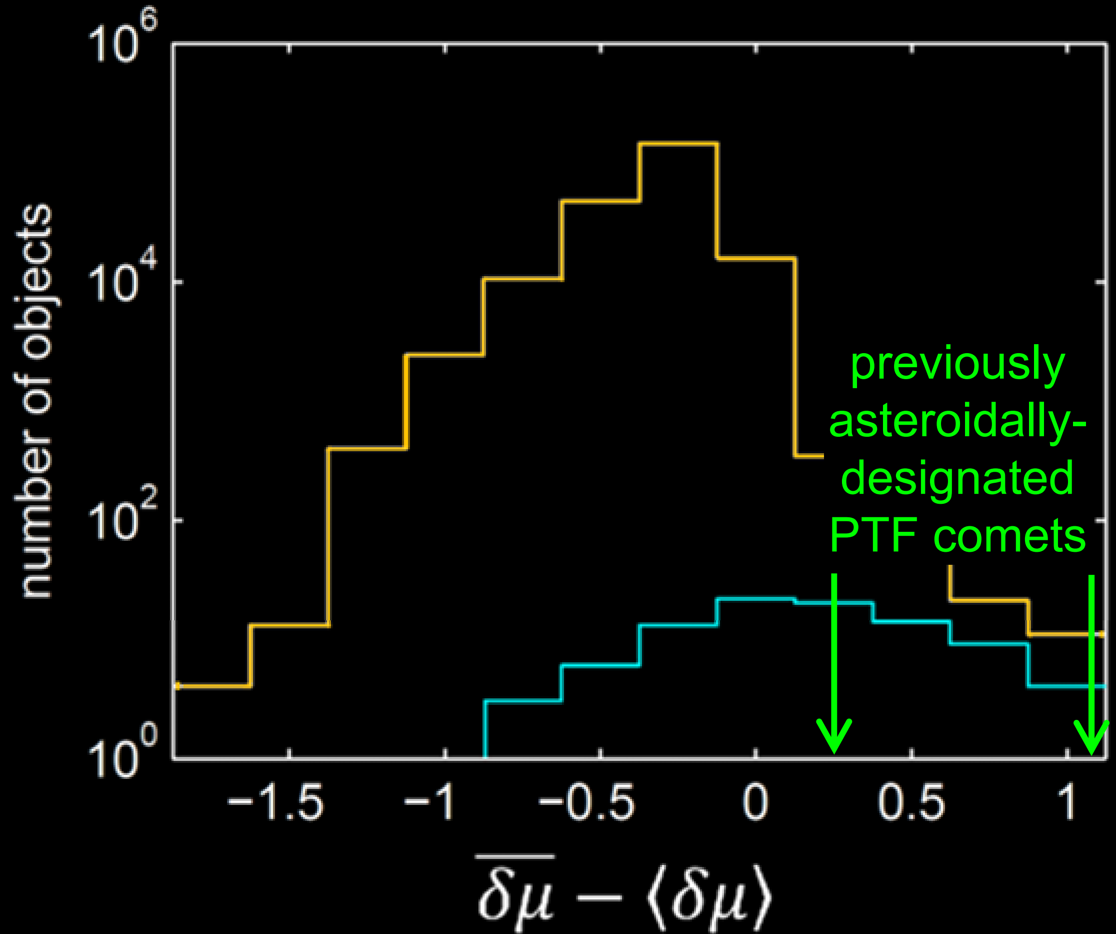

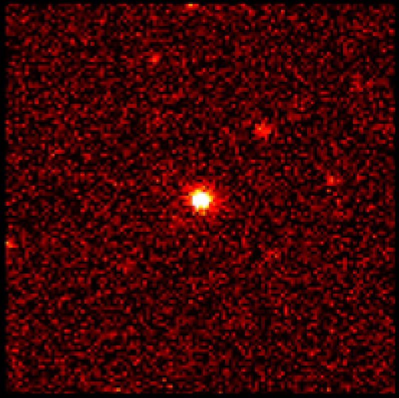

2011 CR42

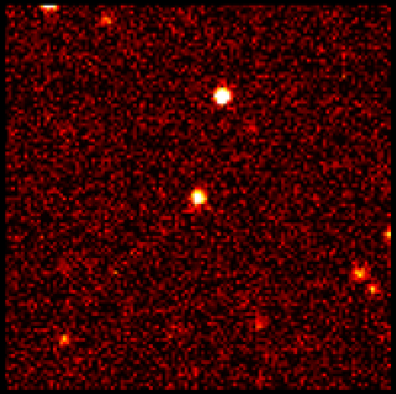

2010 KG43

Quantifying a “cometary” appearance

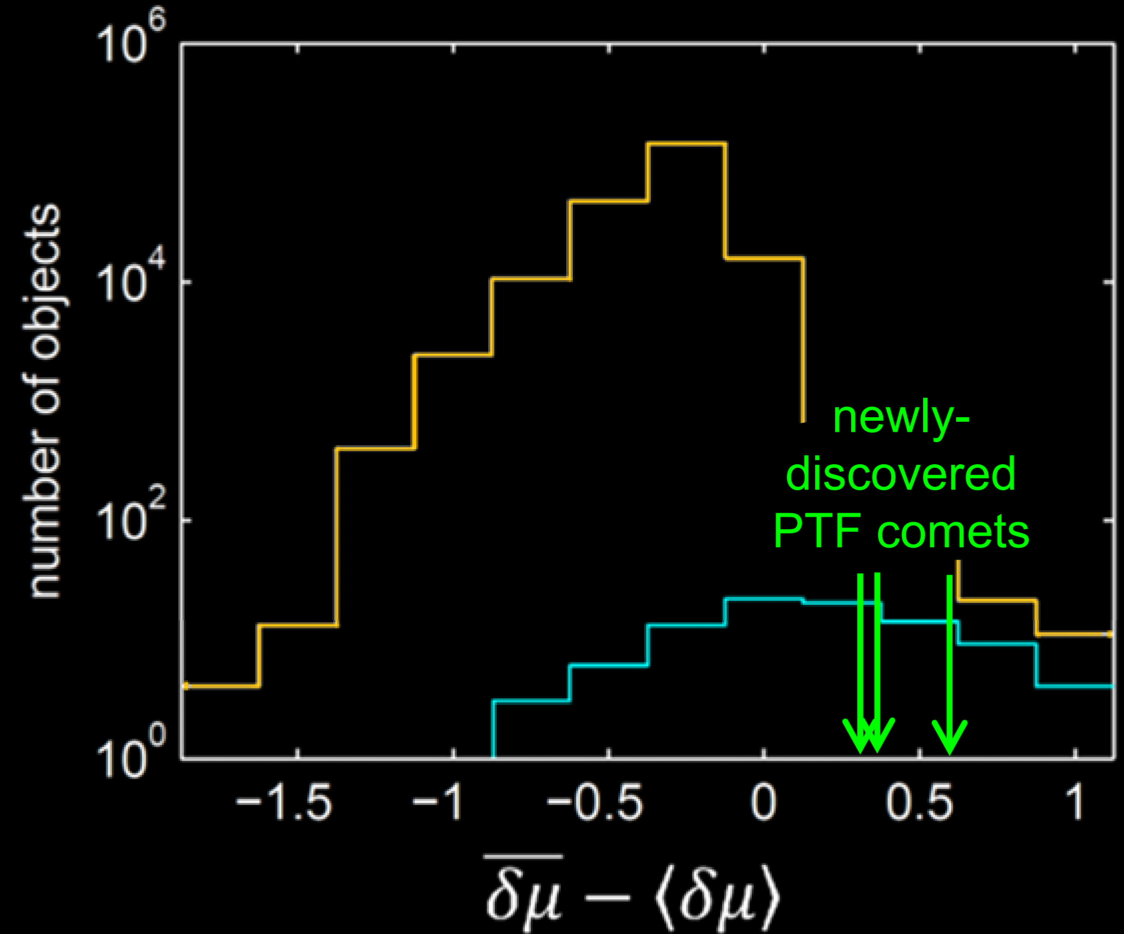

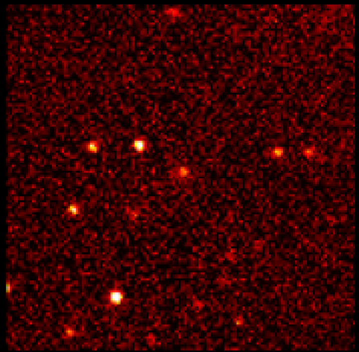

2009 KF37

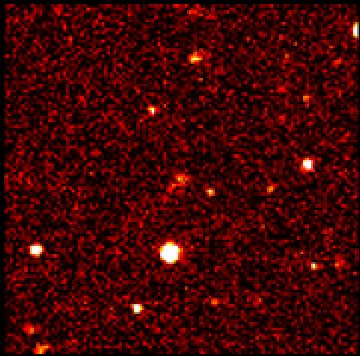

2010 LN135

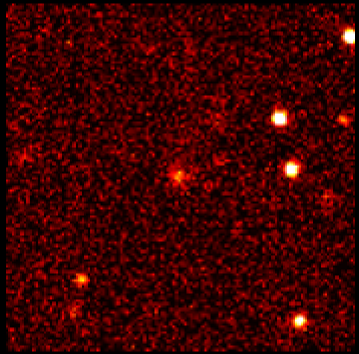

2012 KA51

Statistical analysis

f = true fraction of main−belt objects ($\gtrsim$ 1 km) that are MBCs

$$f_{\min} = \frac{2 \text{ MBCs}}{5 \times 10^5 \text{ main−belt objects}} = 4 \times 10^{-6}$$

S = the PTF sample: 2 MBCs out of $\sim 2.2 \times 10^4$ main−belt objects

Baye's Theorem: $$P(f|S) = \frac{P(S|f) \times P(f)}{P(S)}$$

log−constant prior: $$P(f) = \begin{cases} -\dfrac{1}{f \log(f_{\min})} & f_{\min} < f < 1 \\ 0 & \text{elsewhere} \end{cases}$$

Statistical analysis

$$P(f|S) = \frac{P(S|f) \times P(f)}{P(S)} \qquad P(f) = -\frac{1}{f\log(f_{\min})}$$

C = cometary detection reliability

$n = 2$ = number of MBCs detected in sample S

$N = 2.2 \times 10^4$ = number of main−belt objects in sample S

binomial to Possion: $P(S|f) = \frac{N!}{n!\,(N-n)!}(Cf)^n(1-Cf)^{N-n}$

$$\approx \frac{(NCf)^n}{n!}\exp(-NCf)$$

normalization: $P(S) = \int_{f_{\min}}^{1} P(f)P(S|f)\,df$

Statistical analysis

$$P(f|S) = \frac{f^{n-1}\exp(-NCf)}{\int_{f_{\min}}^{1} f^{n}(1 - Cf)^{N}\,df}$$

$$\propto f^{n-1}\exp(-NCf) \qquad f_{\min} < f < 1$$

Statistical analysis

$$P(f\,|\,S) \propto f^2 \exp(-NCf) \qquad (4/10^6) < f < 1$$

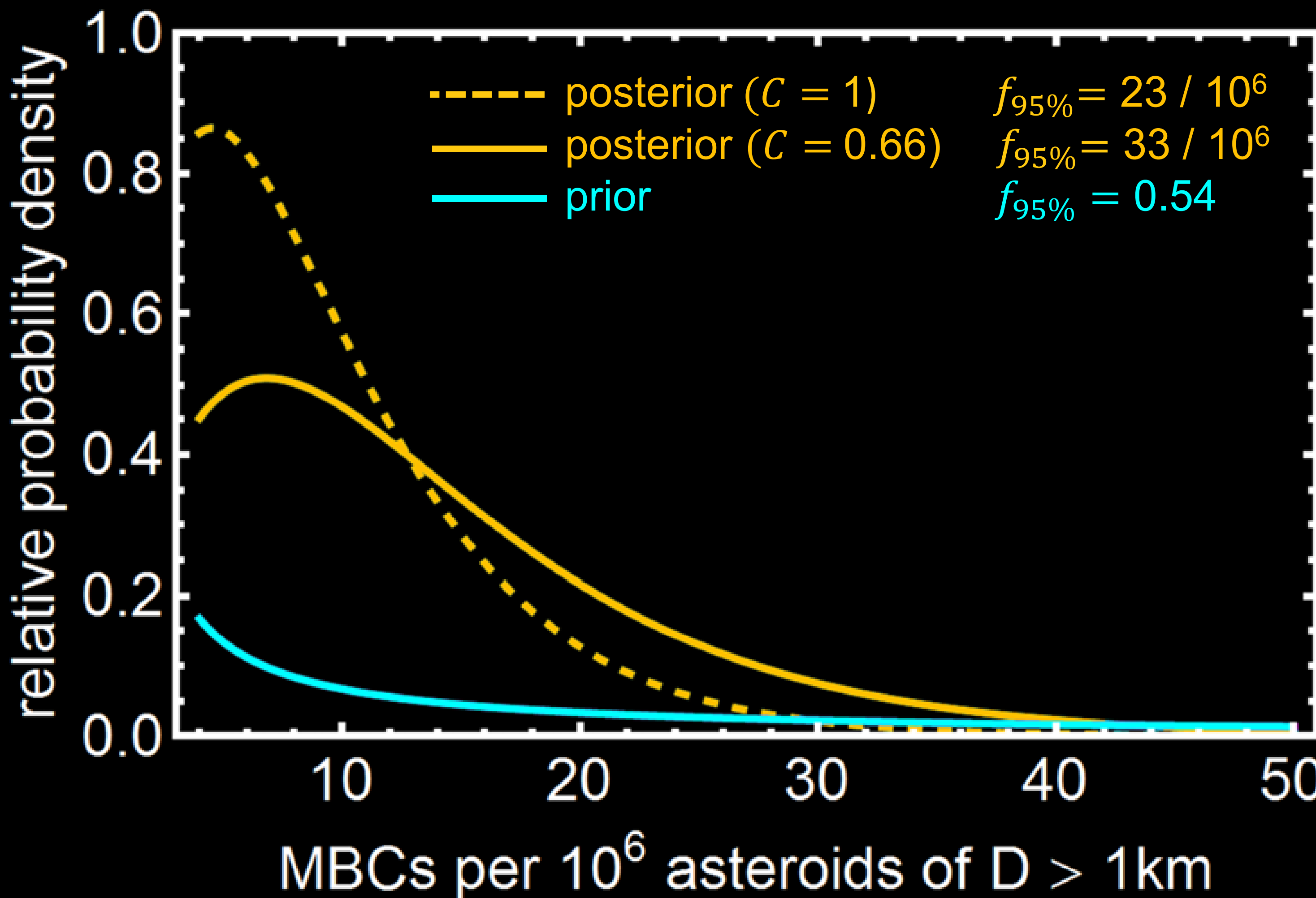

Summary of work

- Our kd-tree-based software efficiently extracts known and new objects
- Our sample contains ~40% of known main-belt objects $\gtrsim$ 1 km in diameter
- Our cometary-detection robustly flags known main-belt comets, and has discovered at least five new (non-main-belt) comets
- For a log-constant prior and 2/3 detection efficiency, our results imply a 95% probability of < 33 MBCs per 10^6 main-belt asteroids

Future work

- Implement orbital-period-baseline photometric variation (including null-detections), possibly incorporating MPC data, as a detection method for unresolved MBCs
- Finish screening of new object discoveries and process post-July-2012 data
- Utilize the PTF dataset for phase-function Hapke modeling